Impacts of battery energy storage technologies and renewable integration on the energy transition in the New York State

Wei-Chieh Huang [a], Qianzhi Zhang [a], Fengqi You [a,b,*]

[a] *Systems Engineering, Cornell University, Ithaca, NY 14853, USA*
[b] *Robert Frederick Smith School of Chemical and Biomolecular Engineering, Cornell University, Ithaca, NY 14853, USA*

ARTICLE INFO

ABSTRACT

In light of current energy policies responding to rapid climate change, much attention has been directed to developing feasible approaches for transitioning energy production from fossil-based resources to renewable energy. Although existing studies analyze regional dispatch of renewable energy sources and capacity planning, they do not fully explore the impacts of the energy storage system technology's technical and economic characteristics on renewable energy integration and energy transition, and the importance of energy storage systems to the energy transition is currently ignored. To fill this gap, we propose an integrated optimal power flow and multi-criteria decision-making model to minimize system cost under operational constraints and evaluate the operational performance of renewable energy technologies with multidimensional criteria. The proposed method can identify the most critical features of energy storage system technologies to enhance renewable energy integration and achieve New York State's climate goals from 2025 to 2040. We discover that lead-acid battery requires an additional 38.66 GW capacity of renewable energy sources than lithium-ion battery to achieve the zero carbon dioxide emissions condition. Based on the cross-sensitivity analysis in the multidimensional evaluation, the vanadium redox flow battery performs the best, and the nickel-cadmium battery performs the worst when reaching the zero carbon dioxide emissions target in 2040. The results of the proposed model can also be conveniently generalized to select ESS technology based on the criteria preferences from RE integration and energy transition studies and serve as a reference for ESS configurations in future energy and power system planning.

1. Introduction

Climate change remediation through the improvement of energy sectors has been pushed into the global agenda, given their low carbon dioxide (CO_2) emissions allowance approved by the Paris Agreement [1]. However, global direct primary energy consumption has doubled from 270.5 EJ in 1978 to 580 EJ in 2018, and fossil-based electricity generation still occupies 85% of the total primary energy consumption [2]. Although the energy transition from fossil fuels to renewable energy (RE) sources is ideally feasible, the integration of RE into the power system is still hindered due to RE's unreliable and intermittent features [3], which makes it difficult to maintain power supplies that are as reliable as fossil-based generators [4]. To achieve the energy transition goal, RE penetration in the power system is inevitable [5]. Therefore, studying the improvement of RE integration in a reliable way has become the current research's focus. Among all the possible solutions to strengthen RE integration, combining RE and energy storage systems (ESSs) [6] has gained the most attention since it systematically and fundamentally stabilizes RE generation by reducing energy dispatch fluctuations [7] and

peak generation pressures [5]. In addition, some studies indicate that the reliance on ESSs is growing significantly along with the increasing RE penetration [8]. For instance, a total of 43 TWh of ESS is required in the national power grid in the United Kingdom to reach 100% RE penetration [9]. Hence, the impact of ESS technology on the power system is tremendous due to its high installation requirements for RE integration. The main factors in ESS technologies that directly affect power system operation can be classified as technical and economic characteristics, which are significantly determined by the materials and mechanisms of ESS technologies [6]. For instance, lithium-ion batteries (LIBs) [10] and sodium-sulfur batteries (NASBs) [11] have different mechanisms and efficiencies for charging and discharging power. Therefore, analyzing the ESS operational performance along with the inherent technical and economic characteristics, such as discharge ratio and capital cost, can provide insights into how different ESS technologies affect power system operations [12] and RE integration strategies [13] to fulfill energy transition goals. Additionally, both ESS's technical and economic properties should be considered critical factors to enhance RE integration considering the ESSs are crucial in supporting RE integration in the energy

Nomenclature

List of Abbreviations

AHP	analytical hierarchy process
BESS	battery energy storage system
CAES	underground compressed air energy storage
CLCPA	Climate Leadership and Community Protection Act
DOD	depth of discharge
EMS	energy management system
ESS	energy storage system
EV	electric vehicle
FES	flywheel energy storage
HES	hydrogen energy storage
LAB	lead-acid battery
LCA	life cycle assessment
LIB	lithium-ion battery
MCDM	multi-criteria decision-making
NASB	sodium-sulfur battery
NGCC	natural gas combined cycle
NGCT	nature gas combustion turbine
NGST	nature gas steam turbine
NICDB	nickel-cadmium battery
NREL	National Renewable Energy Laboratory
NYC	New York City
NYISO	New York Independent System Operator
NYS	New York State
O&M	operation and maintenance
OPF	optimal power flow
PHS	pumped hydro storage
PS	power system
PSB	polysulfide bromine flow battery
RE	renewable energy
RTO	regional transmission organization
SCES	supercapacitor energy storage
SMES	superconducting magnetic energy storage
TES	thermal energy storage
VRFB	vanadium redox flow battery
ZNBRB	Zinc-bromine battery

Sets

B	set of buses
E	set of ESS technologies
L	set of transmission lines
R	set of energy carriers
S	set of load projections
SS	set of scenarios
T	set of timeslots
Y	set of representative years

Parameters

α	line extension factor
BB	susceptance of line (ohm^{-1})
c	unit cost ($/per unit)
D	generator unit CO_2 emissions (ton/MWh)
CEL	annual CO_2 emissions limit (ton)
$\bar{g}$	availability of generators
H	extension/expansion threshold
η	charge/discharge ratio
RP	renewable energy penetration

Continuous variables

N	accumulated cycling numbers
EL	energy level (MW)
C	annual cost ($)
M	installed capacity (MW)

P	power (MWh)
θ	voltage phase Angle (º)

Discrete variables

X	retirement/replacement indicator
z	charge/discharge indicator

Subscripts and superscripts

AP	apparent power
b	bus
cyc	cycling efficiency
disc	discharge efficiency
d	CO_2 emission social cost ($)
e	ESS technology
eis	ESS in-service year
elt	ESS lifetime limit
EC	energy storage system capital cost ($)
EF	energy storage system fix O&M cost ($)
EP	net equipment cost ($)
ER	energy storage system retirement cost ($)
ESS	energy storage system
EV	energy storage system variable O&M cost ($)
EX	existing generator
F	flow
G	generator
GC	generator capital cost ($)
GF	generator fix O&M cost ($)
GR	generator retirement cost ($)
GV	generator variable O&M cost ($)
i, j	transmission line between bus i and j
is	in-service
LD	load
l	transmission line
lmt	limitation
OPR	net operational cost ($)
r	generator carrier
RE	renewable energy
s	load projection
self	self-discharge
ss	scenario
t	timeslot
y	representative year

transition progress. Nevertheless, current studies have not systematically evaluated the effects of ESS technology characteristics on RE integration in power systems [14]. They have also not adequately examined how the energy transition can be achieved with sufficient consideration of those characteristics in different ESS technologies.

Firstly, some existing studies underestimate the impacts of ESS and its technology on RE integration in power systems. For instance, the Spanish regional RE sources are integrated into the national power grid to achieve 49.7% reductions in greenhouse gas emissions [15]. Similarly, Indonesia's regional RE sources have been arranged to achieve 31% RE penetration in 2040 with the cost-minimized objective in the power system [16]. However, they do not consider ESS in their studies. The fact is that ESSs cannot only enhance RE integration in a reliable way but also reduce the same amount of greenhouse gas emissions at an even lower cost by utilizing their storage capacities in the power system. The absence of ESSs may also cause an overestimation of the RE installed capacity needed to achieve a successful energy transition. Secondly, even though some RE integration and energy transition studies consider ESSs, they do not clarify the specific type of different ESS technologies. For example, although the ESSs are implemented to facilitate RE integration [17], the generalized model does not specify the type of ESS technology used in the system. The ESS extensions are considered

in India's national power grid planning to reduce CO_2 emissions by 85% in 2040 without identifying the type of ESS technology [18]. Thirdly, some studies oversimplify the characteristic of various EES technologies, such as [19], only considering simplified battery storage without mentioning the ESS technology characteristics in a big decarbonization project in China. However, due to the diversity of ESS technologies, the absence of explicit descriptions of their characteristics in the RE integration studies may lead to inaccurate results. Fourthly, some studies only consider the limited type and characteristics of ESS technologies for RE integration. The benefits of long-term ESS are discussed to improve RE integration in California [20] but the authors fail to compare the short-term and middle-term ESS benefits. Although pumped hydro storage (PHS) [21] and battery storage [22] have been considered to solve the RE integration in Europe and the U.S., however, the characteristics of battery storage are not clearly explained. Thus, we can argue that other ESS technologies may potentially provide better RE integration strategies due to their higher charging efficiency or lower capital cost. The selection among ESS technologies with distinct characteristics can impact power system operation with high RE integration, which further affects energy transition progress. There is still a noticeable knowledge gap in systematically and comprehensively analyzing the impacts of ESS technology on RE integration and energy transition.

Power system modeling is also critical when investigating the impacts of ESS on RE integration and energy transition. Some studies [23] only consider the system-level power balance constraints, where all the power system facilities, such as generators, ESSs, and demand loads, are connected to a single bus in the power system without spatial information [24]. A system-level or region-level power balance [25] can reduce the computation intensity and provide an energy generation arrangement with the power dispatch strategies to meet the increasing load and RE penetration toward carbon neutrality [26]. The potential of advanced computing technologies in resolving computational difficulties could be significant [27]. In addition, various studies have utilized system-level energy balances to analyze the island and grid-connected operation economic impacts of RE integration [28], the benefits of nuclear flexibility on RE integration in a power system [29], and the ESS role in the future power system [30]. However, geographic and topology information is inaccessible in the above works. Without modeling the transmission lines and buses in a power system model, the required capacities of generators and ESSs may be underestimated due to the insufficient considerations of the transmission distances and power demand distributions through the grid [31]. On the other hand, some studies consider a reduced power system model by incorporating limited geographical information [32]. For example, balancing India's regional demand response and RE sources in only a few selected energy sector sites [33], investigating whole Indonesia's RE sustainability between only five archipelagic states [16], and assessing the RE generation benefits for decarbonization in ten inter-state in the U.S. [34]. However, the topology information used in these studies may be oversimplified, hindering their results' accuracy. Thus, power system modeling with enough topology information [35] should be considered to explore the study of the synergy between RE and ESS in the RE integration and energy transition problems.

Other studies propose different ways for solving RE integration and energy transition problems, such as alternative selections [36] and portfolio planning [37] of RE and ESS. These model frameworks are usually constructed with predefined candidates and portfolios to evaluate the advantages and drawbacks of the ESS technologies and RE sources with multidimensional evaluations using the multiple-criteria decision-making (MCDM) model. The multidimensional evaluations cover extensive metrics for different tasks. For instance, life cycling assessment (LCA) is used to evaluate the sustainability of RE technologies [38]. Technical [39] and economic metrics are used to evaluate RE and ESS selection [40] with Shannon entropy [41] and analytical hierarchy process (AHP) [42,43]. Although these MCDM models provide a consistent basis for ESS technology comparisons and optimize the selection from

multiple criteria [44], the evaluations of ESS technologies in the above works may be biased because they do not involve power system modeling and apply the constraints of energy transition goals. Besides, these works incorporate many metrics that do not directly affect power system operation, such as social acceptance. Therefore, the highly prioritized ESS technologies in the previous MCDM studies may not always lead to the optimal selection in the power system operation optimization model for RE integration. For example, studies indicate that LIB is the prioritized ESS technology in the resident stationary grids [45] based on their inherent characteristics and consumer acceptance. However, due to the significantly high unit capital cost compared to other ESS technologies [46], LIB may not be favored in the power system operation optimization model. On the other hand, without the multidimensional evaluations from the MCDM model, the single-layer optimization can only provide the optimal solution from a single dimension, limiting the selection of ESS technology in the RE integration problem and hindering the RE integration and energy transition development.

To fulfill the aforementioned research gaps of existing studies, we propose an integrated OPF-MCDM (optimal power flow-multiple criteria decision-making) model, which includes two parts: the OPF part [47] defines power flow transmission and bus-level power balance constraints and provides a system-level optimal solution; the MCDM part evaluates ESS technologies from multidimensional perspectives by importing the OPF results and the inherent characteristics of various ESS technologies, which can evaluate the performance of the selected ESS technologies for RE integration and energy transition. In this study, we conduct a case study in New York State (NYS), which cover the stage-wise climate goals as defined by Climate Leadership and Community Protection Act (CLCPA) [48]. Our comprehensive future scenario design with the NYS case study can help the proposed OPF-MCDM model to determine the proper ESS technology for RE integration and energy transition over a long-time horizon. It is worth noting that the scope between this study and the previous study [49] is different, and the studies support the energy transition in NYS from different perspectives. The previous study [49] implemented robust optimization to evaluate the RE integration progress under uncertainty, which is an important issue in power generation systems [50]. They do not consider the power transmission network in the power system modeling and do not consider the expansion of ESS technology in NYS. In this work, the aim is to evaluate the impact of ESS technology on the RE integration and energy transition in NYS with stage-wise energy transition and climate goals. We consider the power transmission network in the power system modeling. The future scenario design covers certain uncertainties, the stage-wise energy transition and climate goals, the ESS technology development impact on cost reduction, the policy restriction of CO2 emissions, the different load projections, and the dispatchable RE concept. The results can give general suggestions for the ESS technology selections based on their criteria preference for future energy transition studies.

The main contributions of this work are summarized as follows:

- Six ESS technologies' impacts on NYS power transmission system operation with stage-wise RE integration and energy transition targets are fully investigated. Based on the spatial and temporal analysis, the most critical features of ESS technologies are identified to enhance RE integration and achieve NYS's climate goals.
- The proposed future scenario design from 2025 to 2040 thoroughly explores the ESS technology developments, power system evolutions, climate goals, the drought impact, and the price changes of generator dispatches, ESS technologies, and CO_2 emissions.
- A novel integrated OPF-MCDM model is proposed to quantify the performance of ESS-related OPF solutions under multidimensional evaluations. The proposed OPF-MCDM model provides more flexibility in selecting ESS technologies based on different technical, economic, and operation preferences for RE integration and energy transition.

The remainder of the paper is constructed as follows: We illustrate the problem statement of this study in Section 2. In Section 3, we demonstrate the methodology of this study and the research framework arrangement, which includes the future scenario design, power transmission system modeling, the OPF model formulation, and the OPF-MCDM evaluation process. Section 4 describes and discusses the results of the OPF-MCDM model evaluation on the NYS power system and ESS technology selection impact by criteria. In Section 5, we present the conclusions of this study.

2. Problem statement

In this work, we propose an integrated OPF-MCDM model with future scenarios from 2025 to 2040 in the NYS power transmission system to quantify the impacts of ESS technologies with distinct technical and economic characteristics on RE integration and energy transition. The future scenario design combines the load projection variances, the stage-wise climate goals, the six selected ESS technologies with future developments, and the CO_2 emission restrictions. The input data comprise the initial information about the capacities of generators, ESSs, and loads, the targets of RE integration and energy transition, the economic and technical characteristics of ESS technologies, the corresponding economic data of generators and ESS technologies, and the economic data of CO_2 emissions cost. The decision variables of the OPF model include the installation and operations of the generators, ESS, and lines. The OPF model aims to minimize the annual power system cost and obtain the optimal RE integration and energy transition pathway. The OPF solution is delivered to the MCDM model and evaluated together with the ESS technology's inherent characteristics for the performance evaluation in the pathway toward energy transition with a uniform scale and multi-dimensional preferences. The output of the OPF-MCDM model includes the performance of different ESS technologies in different scenarios to show the selection priority of ESS technologies for RE integration and energy transition. The overall framework of the OPF-MCDM model is described in Section 3.3. The compact OPF formulation and detailed OPF constraints can be found in Section 3.2 and Appendix B.1, B.2, B.3, and B.4, respectively.

3. Methodology

3.1. Systems modeling and optimization framework

The overall framework of the proposed method is illustrated in Fig. 1. First, we collect the ESS technology's technical and economic characteristics from the recent ESS reviews [51] of development [52] with life cycle analysis [53–55] and ESS application reviews of versatile [46], utility-scale [56] and grid-connected implementation [57], to illustrate the reasons for selecting the ESS technology and their future costs. The underlying considerations for selecting ESS technologies, technical and economic characteristics, and the future cost simulations of ESS are described in Appendix A. Based on the literature review, we select six scalable ESS technologies, including LIB, NASB, lead-acid battery (LAB), nickel-cadmium battery (NICDB), vanadium redox flow battery (VRFB), and Zinc-bromine battery (ZNBRB). These six technologies can also be classified as the battery energy storage system (BESS), although we acknowledge there are many other energy storage technologies and options [58,59] that are not considered in this study. Then, we construct a power transmission system model in NYS, including the transmission lines, generators, and loads based on the high-fidelity data collection from the New York Independent System Operator (NYISO)'s report [60], system map [61] and power market data [62]. The future scenarios of RE integration and energy transition in NYS are designed with the stage-wise climate goals defined by the CLCPA [48], the clean energy standards [63], the future load projections [48], and the selected BESS technologies. We also consider the future scenarios of the generators' development and ESSs' impact [64] on capital, O&M cost, retirement,

and replacement cost, the restriction of CO_2 emission impact on the social cost [65], and dispatchable RE concept fulfilled by the ESS [66], uncertainty RE generation [67], regional synergy [68], algorithm [69], and smart grid control [70]. Lastly, an OPF problem is formulated and solved by the Pyomo package with the Gurobi solver. The MCDM model receives the OPF solution and ESS inherent characteristics to generate the performance scores of the BESS technologies by scenarios. Here, the performance score quantifies the selection priority of BESS technologies under technical, economic, and operational preferences. The higher performance score represents that this BESS technology outperforms the others.

3.2. Introduction of the future scenario design, New York State power transmission system modeling, and optimal power flow formulation

In response to the energy transition and climate goals within the U.S. and the signing of the CLCPA into law [48], the NYS government established stage-wise climate goals to facilitate RE integration and energy transition in NYS from 2025 to 2040. The milestones of RE integration and climate goal can be partitioned into four main stages: (1) The installed capacity of distributed solar will reach 6000 MW by 2025. (2) The installed capacities of ESS and distributed solar capacity will reach 3000 MW and 10,000 MW by 2030, respectively. The overall RE production, including distributed solar, onshore wind power, and offshore wind power, will account for 70% of the annual energy production by 2030 [71]. (3) The installed capacity of offshore wind power will reach 9000 MW by 2035. (4) Energy production with zero CO_2 emissions will be reached by 2040 [48]. These four stage-wise climate goals are represented by four representative years, 2025, 2030, 2035, and 2040 to perform the temporal analysis conducted in the future scenario design. The current installed capacities of distributed solar energy, onshore wind power, offshore wind power, and ESS are low, but they will have significant increment to support the energy transition in the following decades. It is worth noting that as per 2022′s load and capacity book [60], distributed solar energy, onshore wind power, and offshore wind power have grid-connected capacities of 76.5 MW, 2191.5 MW, and 0 MW, respectively. Onshore wind power is the renewable energy with more development in the NYS power system compared to distributed solar and offshore wind power. The offshore wind power plant is under construction and will be available in the following years. This study only focuses on renewable solar and wind power and does not consider other promising RE technologies that have great promises for power generation in NYS, such as geothermal [72,73]. In addition, NYS's grid-connected ESS installed capacity is 638 MW in 2022, with a high escalation rate in the following decades to support the energy transition toward zero carbon emissions in 2040. In addition, we also consider the developments of technology and energy policy in the future scenario design, including the future capital, O&M, and retirement costs of the generators and ESS technologies [64], the load projections [48], the restrictions of CO_2 emission [65,74], and the concept of dispatchable RE [66,68–70,75]. The objective of this comprehensive future scenario design is to cover the extensive future variances of the ESS technology for RE integration and energy transition from 2025 to 2040 in the NYS power transmission systems.

Based on the latest public access information, we establish a county-level NYS power transmission system model and adjust the inner bus connections following the topology information from the 2019 NYS power system map [61]. In addition, the generators' location, capacity, and carrier are collected from the 2022 Load & Capacity Data Gold Book [60]. The 2019 hourly load data is extracted from NYISO's energy market & operational data [62] and scaled based on the load projection ratio of each representative year. This NYS power transmission system model includes 121 buses, 698 generators, and 184 transmission lines, as shown in Fig. 1. The standard voltage levels of the transmission lines include 115, 138, 230, 345, and 765 kV in the NYS power system [61]. Because of the lack of specifications for the low-voltage transmis-
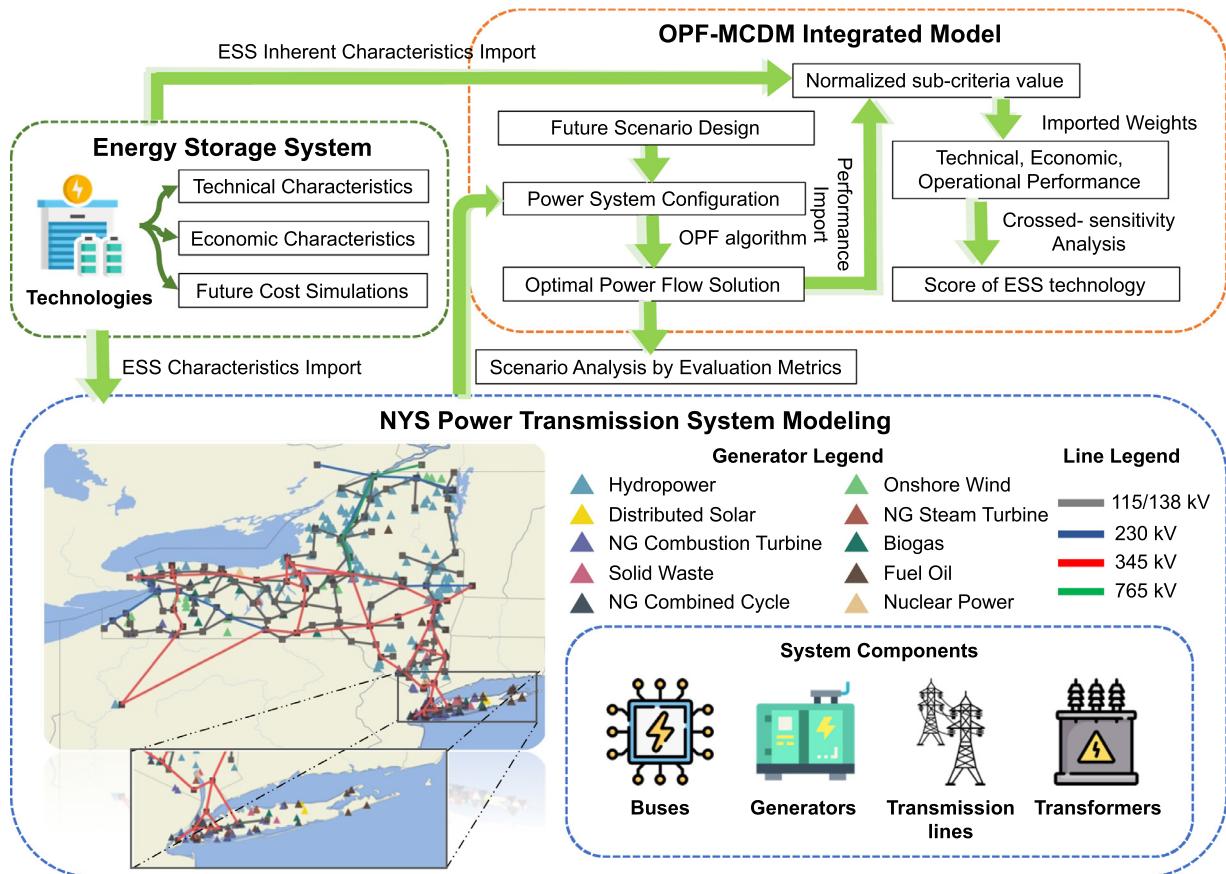
Fig. 1. The overall framework of this study includes three parts: the energy storage system, New York State power transmission system modeling, and the optimal power flow-multiple-criteria decision-making model.

sion lines on the map, the voltage level under 230 kV is assumed to be 138 kV.

NYISO partitioned the NYS territory into 11 control zones, from A to K [76,77], to maintain the complex power system market. In this study, zones J and K are the heavily loaded zones due to their high population near New York City (NYC). The other zones are regarded as lightly loaded zones. We focus on analyzing the installation and operational performance of REs and ESSs between heavily loaded and lightly loaded zones to understand the selection of ESSs to accelerate the RE integration and energy transition in NYS.

This study performs the optimization with objective and operational constraints in the OPF model. The transmission line's reliable reactive power information is unavailable; thus, our OPF model concentrates on a DCOPF model rather than an ACOPF model. Extension to an ACOPF model is possible if the reactive power information is available. The objective of this DCOPF model is to minimize the total power system cost on a yearly basis, as described in Eq. (1). The constraints of the generators, ESSs, network operations, and annual CO_2 and RE production can be found by referring to Sections B.1, B.2, B.3, and B.4 in Appendix B, respectively.

$$\min obj_{ss} = C_{ss}^{EP} + C_{ss}^{OPR}, \forall ss \in SS \quad (1)$$

s.t. Generator constraints (B1)-(B7);
    Energy storage system constraints (B8)-(B15);
    Network operational constraints (B16)-(B20);
    Annual CO_2 and RE production constraints (B21)-(B22).

The annual total power system cost in Eq. (1) includes the annual net equipment cost C_{ss}^{EP} and the net operation cost C_{ss}^{OPR} in each scenario ss. The set SS can be represented as a combination of $[E, S, Y]$,

where E represents the set of BESS technologies e, S denotes the set of load projections s, and Y represents the set of representative years y with different climate goals in NYS. The annual net equipment cost C^{EP} and operation cost C^{OPR} can be obtained in Eqs. (2) and (3), respectively.

$$C_{ss}^{EP} = C_{ss}^{GC} + C_{ss}^{EC} + C_{ss}^{GR} + C_{ss}^{ER} + C_{ss}^{l}, \forall ss \in SS \quad (2)$$

where the annual net equipment cost C^{EP} includes the annual generator capital cost C^{GC}, annual ESS capital cost C^{EC}, generator retirement cost C^{GR}, ESS replacement cost C^{ER}, and transmission line extension cost C^l.

$$C_{ss}^{OPR} = C_{ss}^{GF} + C_{ss}^{GV} + C_{ss}^{EF} + C_{ss}^{EV}, \forall ss \in SS \quad (3)$$

where the annual operation cost C^{OPR} composites the annual generator fixed O&M cost C^{GF}, annual generator variable O&M cost C^{GV}, annual ESS fixed O&M cost C^{EF}, and annual ESS variable O&M cost C^{EV}.

3.3. Flowchart and evaluation criteria of the integrated optimal power flow – multi-criteria decision-making model

After we solve the OPF problem, the optimal solution is delivered to the MCDM model, following the steps and computational settings in Fig. 2. First, the selected BESS technology characteristics and loads from the selected projection of the initial representative year 2025 are integrated into the OPF model to obtain the optimal solution of the generators' dispatches, power flows and installation strategies of ESSs and RE sources. The performance of BESS technology from the OPF solution and the BESS technology's inherent characteristics are delivered to the MDCM model to acquire the performance scores of the BESS technologies by scenario. Then, the installed capacities of ESSs and RE sources are determined to update the following representative year's initial RE
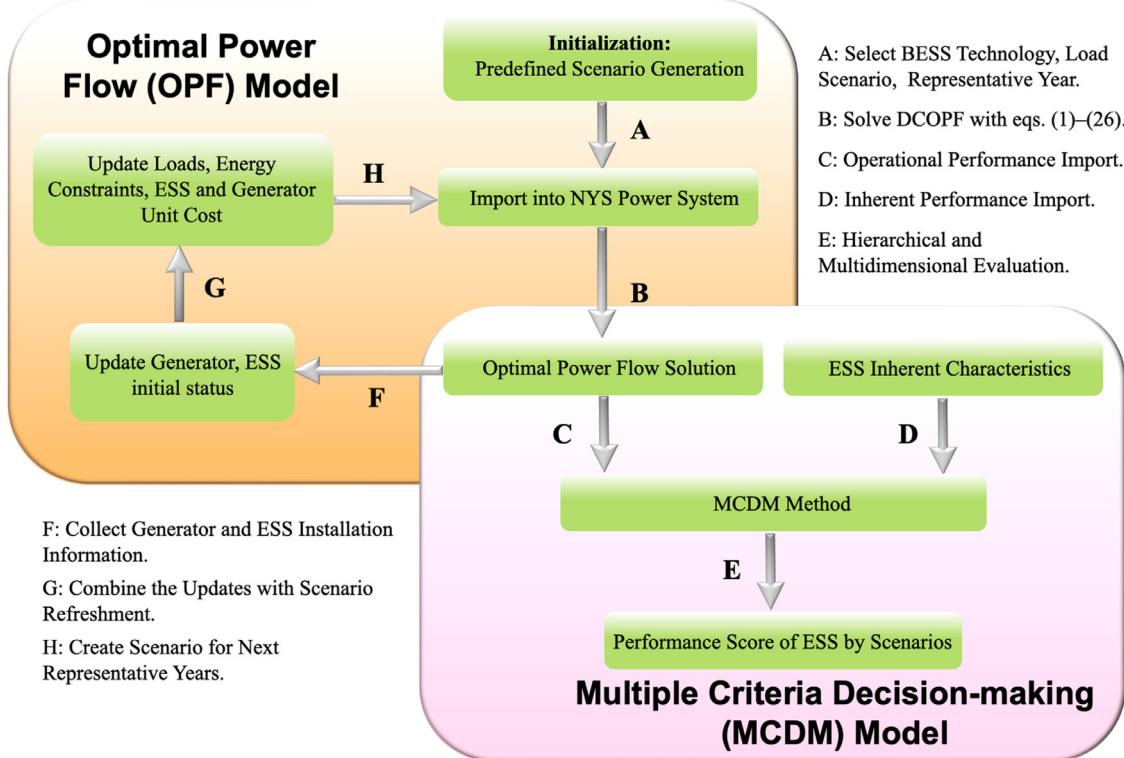
Fig. 2. Flowchart of the proposed OPF-MCDM model. The OPF model generates the optimal power flow solution, and the MCDM model is responsible for calculating the performance scores of the selected BESS technologies.
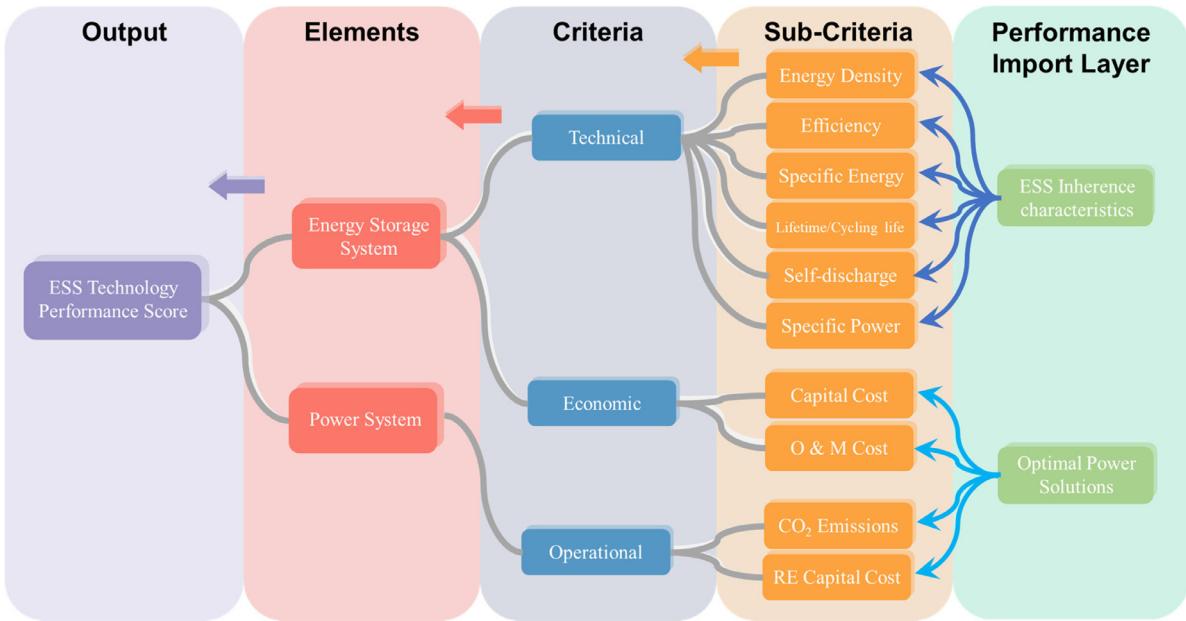
Fig. 3. The multidimensional criteria evaluation process consists of five layers. The inputs from the performance import layer are normalized in the sub-criteria layer and multiplied by the weights or ratios in each layer to ultimately obtain the ESS technology's performance score.

and ESS conditions. In the next representative year, the OPF model is solved with the updated RE and ESS status to obtain the OPF solution with a new climate goal. This iterative process continues until all four representative years of BESS technology e in load scenario s are covered.

After solving the OPF model, the selected BESS technology's operational and installation performance will be delivered to the MCDM model for evaluation with multidimensional criteria. The evaluation criteria and the hierarchical structure of the MCDM model are denoted in

Fig. 3. The MCDM model comprises the performance import layer, sub-criteria layer, criteria layer, elements layer, and output layer. Specifically, we review the previous MCDM studies on the ESS technologies to support us in selecting the metrics. We aim to include more metrics related to the power system in the evaluation to make the process more comprehensive. Through the review, we discover some features, such as energy density, efficiency, cycling, and lifetime, that are critical for selecting ESS technology. Therefore, we select ten matrices in

the sub-criteria under the preference of technical, economic, and operational criteria. It is worth noting that the metrics in the social aspects are not considered because the value may have significant diversity and is not directly related to the power system operation [78]. Chosen metrics can refer to Fig. 3 for more details. The metrics include (1) energy density, the energy density of ESS technology; (2) efficiency, the average of cycling and discharge efficiency; (3) specific energy, the specific energy of the ESS technology; (4) lifetime/cycling life, the length of time the ESS can be used and their cycling limits; (5) self-discharge, the self-discharge rate of the ESS technology; (6) specific power, the specific power of ESS technology; (7) capital cost, the annual total capital cost of ESS; (8) O&M cost, the sum of annual ESS fixed and variable O&M cost; (9) CO_2 emissions, which are caused by generators during operation; and (10) RE capital cost, the annual RE installation cost. The sub-criteria (1)–(6) come from the inherent characteristics of ESS technologies, and sub-criteria (7)–(10) come from the optimal power flow. The metrics are determined by following the investigation of the most crucial metrics obtained from the previous study [79]. In addition, we include the metrics of power system operation and RE integration [41], such as RE capital cost and CO_2 emissions, which are impacted by the different BESS technologies in our study. For calculation, the sub-criteria performance values are first normalized to a uniform scale to reduce the calculation variance and then multiplied by the weights adopted from previous MCDM studies [41,79], as shown in Table 3. The sum products of weights and the sub-criteria value are aggregated to the technical, economic, and operational performance values in the criteria layer. The values in the criteria layer of each representative year are averaged to reduce the complexity of the multidimensional evaluation. Furthermore, to evaluate the impact of weight change on the criteria, we implement the cross-sensitivity analysis on the weights of the technical, economic, and operational criteria. Namely, two ratios are considered for the cross-sensitivity analysis: the technical-economic ratio between the technical and economic criteria; and the Power System (PS)-ESS ratio between the ESS and the operational performance in the elements layer.

4. Results and discussions of the New York State case study

This section gives the ESS performance, RE integration, and energy transition results in the NYS case study to demonstrate the correctness of the proposed OPF-MCDM model for analyzing the BESS technology impact on the RE integration and energy transition. This case study conducts a comprehensive scenario analysis of six selected BESS technologies, four representative years with climate goals from the CLCPA [48], and three load projections from the NYISO report [48]. The spatial distribution of load is collected from historical data [62] in the pre-Covid-19-pandemic year 2019, considering the load may be untypical in the Covide-19 pandemic year. If we consider the load condition in 2019 as a reference basis, the high load projections for 2025, 2030, 2035, and 2040 are 101%, 106%, 122%, and 139% of the reference basis, respectively. The medium load projections for 2025, 2030, 2035, and 2040 are 96%, 96%, 107%, and 118% of the reference basis, respectively. The low load projections for 2025, 2030, 2035, and 2040 are 93%, 90%, 95%, and 102% of the reference basis, respectively. The four representative years with the corresponding stage-wise climate goals are presented in Table 1, and the projection ratios with corresponding loading conditions are described in Table 2. The scenarios combine six BESS technologies, three load projections, and four representative years to sum up 72 scenarios.

The OPF model is built by the PyPSA package [80]. The hourly loads are scaled based on the load increments between the representative years. The interface transmission data is collected from the NYISO energy market & operational data [62]. There are 11 types of generator carriers considered in this case study of NYS power systems, including biogas, distributed solar, fuel oil, hydropower, natural gas combined cycle (NGCC), nature gas combustion turbine (NGCT), nature gas steam turbine (NGST), nuclear power, onshore wind power, offshore wind power, and solid waste. The grid-connected behind-the-meter (BTM) data is collected from the NYISO load & capacity gold book [60]. In the energy carriers, only distributed solar, onshore wind, and offshore wind power are extendable to achieve the energy transition. We also notice that drought has happened more frequently in recent years and can potentially impact future hydrogen power generation. Therefore, we assume hydrogen power generation reduce by 30% in all the scenarios to simulate future drought impact. In addition, the generator capacity extension data is adopted from the CARIS report [81,82]. We collect the generation's future capital, operational, and retirement cost data by carriers. The line characteristics of the transmission lines follow the PyPSA package standard [83]. We assume the initial capacities of the transmission lines follow the surge impedance loading [84] and the peak demand by zone [60], with fourth times the extension threshold to cover the increasing load and RE penetration across NYS. In terms of ESS capacity, 50% of the capacity extension threshold is considered from 2025 to 2035. Moreover, considering the drought impact on hydrogen power generation, the strict zero carbon dioxide emissions goals, and the high demand loads, 270% capacity extension thresholds are applied to the ESS as the constraint to restrict the ESS capacity extension within a reasonable range. We also assume that ESSs shall be installed near the top three densely populated locations in each zone to respond rapidly to the high demand loads. However, the candidate locations for ESS installation are distributed across NYS, making the locational environments vary significantly by weather conditions and increasing the complexity of the optimization problem. Thus, we follow the degradation evaluation of ESS from previous studies [85,86] for simplification. Similarly, the transformer capacity is not considered in this study.

To validate the OPF model, we compare our results with the expected energy capacity extension [87] from NYISO published report. This report shows that NYS's total installed capacity of generators is projected to be approximately 50, 65, 81, and 112 GW in 2025, 2030, 2035, and 2040, respectively. In our simulation results, the average installed capacities of generators are 50.2, 69.8, 79.1, and 115.5 GW between different BESS technologies. The annual estimated installed capacities of generators are similar to the NYISO's predictions.

In the MCDM model, we adopt the sub-criteria weights from the previous MCDM studies, as shown in Table 3. Those weights are normalized, and the summation of weights equals to 1.0 in each criteria. In addition, the cross-sensitivity analysis between the criteria layer, element layer, and objective layer with the technical-economic ratio and PS-ESS ratio have values ranging from 0.1 to 0.9, which can help us to understand how ESS technology selection priority varies with the different combinations of criteria preferences.

Section 4.1 presents ESS and RE's installed capacities and the regional distribution of generator installed capacity between BESS technologies. The observation from these comparisons brings out the discussion of which BESS technology required less installed capacities of ESS and RE to achieve the same climate goals and what is RE installed capacity location preference for ESS. The discussion can help us realize the synergy between ESS and RE to enhance the RE integration and energy transition. Section 4.2 presents the operational result of different BESS technologies under different scenarios. The observation that the BESS technology performs differently on cycling numbers, CO2 emissions, and the total system cost render the systematic perspectives of what kind of BESS technology may have better operational performance under different scenarios with various climate goals. Section 4.3 presents the multidimensional evaluation results of BESS technologies from the OPF-MCDM model. The observation of how the performance score of BESS technologies varies under different combinations of criteria preferences and scenarios is presented in this section. This observation is discussed by scenarios, BESS technologies, and different criteria preferences, and gives the general suggestion of the BESS technology for RE integration and energy transition problem.

Table 1
RE integration and climate goals in four representative years, 2025, 2030, 2035, and 2040.

Representative Years	RE integration and climate goals
2025	The installed capacity of distributed solar reaches 6000 MW.
2030	(1) The installed capacity of ESS reaches 3000 MW. (2) The installed capacity of distributed solar reaches 10,000 MW. (3) RE energy production, including distributed solar, onshore wind power, and offshore wind power, accounts for 70% of the annual energy production.
2035	(1) The installed capacity of offshore wind power reaches 9000 MW. (2) CO_2 emissions are assumed to be at most half the level in 2030 to achieve zero CO_2 emissions in 2040.
2040	The goal of energy production with zero CO_2 emissions is achieved in this representative year.

Table 2
Three load scenarios, high, medium, and low, in each representative year and their corresponding ratios compared to the 2019 reference load level [48].

Load Scenario	2025	2030	2035	2040
High	101%	106%	122%	139%
Medium	96%	96%	107%	118%
Low	93%	90%*	95%	102%

* Low load scenario in 2030 assumes high adoption of energy efficiency measures and behind-the-meter solar energy, which decreases the demand loads.

Table 3
The selected metrics in the sub-criteria layer are related to the BESS technologies and the power system operation performance. The weights of the metrics in the sub-criteria layer are adopted from the RE [41] and ESS [79] selection studies and normalized for calculation purposes.

Elements	Criteria	Sub-Criteria (metrics)	Weights
Energy Storage System	Technical	Energy Density	0.2426
		Efficiency	0.1270
		Specific Energy	0.1905
		Lifetime/Cycling Life	0.1202
		Self-discharge	0.1293
		Specific Power	0.1904
	Economic	ESS Capital Cost	0.5294
		ESS O&M Cost	0.4706
Power System	Operational	CO_2 Emissions	0.7547
		RE Capital Cost	0.2453

4.1. Spatial and temporal analysis of energy storage system technology selection and renewable energy installation

We first notice ESS's installed capacities and operational differences among BESS technologies when analyzing the results from the OPF-MCDM model. In order to show the most paradigmatic differences between BESS technologies, we select the four most representative BESS technologies in the high projection out of the total 72 scenarios for visualization in Figs. 4 and 5: (1) LIB, the most commonly used BESS technology; (2) LAB, a BESS technology in conservative innovation scenario; (3) VRFB, a BESS technology in the advanced innovation scenario; (4) NASB, the technology in the moderate innovation scenario. Fig. 4 illustrates the zonal installed capacities and the cycling numbers of those four selected BESS technologies with high load projections in 2025, 2030, 2035, and 2040. A, B, C, and so on in the *x*-axis in Fig. 4 represents the control zones in NYS.

In Fig. 4, the lines represent the ESS's installed capacity in MW in different zones, and the bars represent the cycling numbers of ESS in different zones. Note that the cycling numbers of ESS will be discussed in Section 4.2 with the analysis of total system costs and CO_2 emissions. From the observation of Fig. 4, we discover that the installed capacity of each BESS technology increases significantly as the RE penetration increases, from an average installed capacity of 1.85 GW in 2025 to 25.3 GW in 2040 among all BESS technologies. The installed capacities of the four BESS technologies are close to the baseline extension (0%) in 2025, while the installed capacities of the four BESS technologies are close to the extension limit (270%) in 2040, as shown in Fig. 4(a) and (d), respectively. The main reason for this tendency is that there are relatively low loads and low RE penetration with the high capital cost of BESS technologies in 2025. In contrast, the loads and RE penetration are high, with relatively low ESS capital of BESS technologies in 2040. The trend of ESS installed capacity preference from the baseline (0%) in 2025 to the extension limit (270%) in 2040 indicates that more ESS installed capacity benefits the RE integration in the power system, especially when in the high RE penetration condition.

Moreover, we discover that the ESS installed capacity differs greatly from BESS technologies. As shown in Fig. 4(a)-(d), LIB has the ESS installed capacities of 1.85 GW, 6.94 GW, 6.97 GW, and 25.86 GW in 2025, 2030, 2035, and 2040, respectively. The lowest ESS installed capacity for LIB among BESS technologies is due to its high cycling efficiency, low self-discharge ratio, and high capital cost. LAB has a worse cycling efficiency than LIB, with a value of 76.5%, a low capital cost, low maximum depth of discharge (DOD), and low discharge time among BESS technologies. Thus, LAB has much more ESS installed capacities than LIB, with capacities of 1.85 GW, 7.88 GW, 11.61 GW, and 25.86 GW in 2025, 2030, 2035, and 2040, respectively. Fig. 4(c) shows that VRFB has a high ESS installed capacity of approximately 11.61 GW because of its lower efficiency and lower capital cost than LIB. NASB presents a similar pattern to LIB, with a capacity of 6.53 GW due to the high efficiency and the high capital cost, as shown in Fig. 4(c). As shown in Fig. 4(b)-(d), LAB, with the lowest efficiency, lowest maximum DOD, and lower discharge time, has additional 940, 4640, and 7.2 MW ESS installed capacities than LIB in 2030, 2035, and 2040, respectively. From the above observation, we can conclude that the BESS technologies, with no matter lower charge-discharge efficiencies, lower maximum DOD, or lower discharge time, require an additional installed capacity of ESS to achieve the same climate goals compared to other BESS technologies. Furthermore, these ESS installed capacity differences between BESS technologies are significant, especially with the high RE penetration.

When we break down the zonal level observation in Fig. 4, it can be found that ESS installed capacity is also different between control zones. As shown in Fig. 4(a)-(d), lightly loaded zones A, B, D, and E have ESS installed capacities typically close to the extension limit. In contrast,
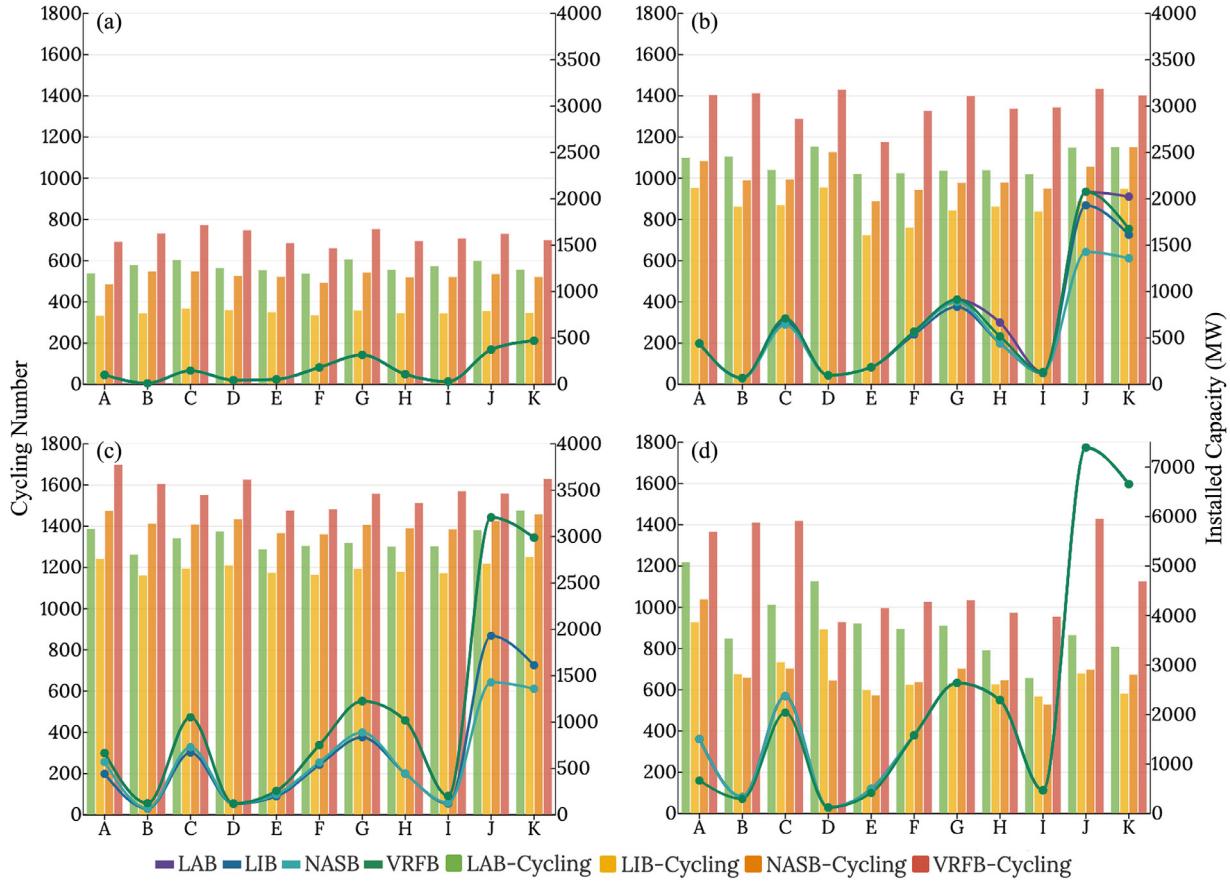
Fig. 4. The zonal installed capacities (lines) and total cycling numbers (bars) of BESS technologies with high load projections in the four representative years: (a) 2025, (b) 2030, (c) 2035, and (d) 2040.

heavily loaded zones J and K mostly have ESS installed capacities that do not reach the extension limit. The ESS installed capacities close to the extension limit represent the ESSs in the lightly loaded areas are crucial and cannot be ignored. The main reason for causing the preference is the synergy between ESS and RE in the unbalanced load distribution region. Loads in the NYS power system are highly unbalanced distributed. The total load in the areas of Bronx, NYC, Kings, Queens, Richmond, Nassau, and Suffolk, the seven counties in zones J and K out of 62 counties in NYS, accounts for 57.4% of the total load in NYS. Since the demand loads in the lightly loaded areas are low, the distributed ESS can store the additional RE production in diversified locations. Besides, the high ESS installed capacity for these distributed ESSs can significantly enhance the reliability of the power system operation due to their high volume to conduct energy redistribution and avoid transmission congestion. In contrast, RE production is usually used to supply the high local demand loads in the heavily loaded areas, which can reduce reliance on the ESSs. Therefore, there is less ESS installed capacity preference in the heavily loaded area. A similar tendency can be observed in the latter discussion of the zonal RE installed capacity differences.

The installed capacities of the generators with four representative BESS technologies and high load projections in 2025, 2030, 2035, and 2040 are presented in Fig. 5. Those generators have 11 different energy carriers with the two additional energy sources, the imported energy, and the BTM energy generation, as mentioned in Section 4. From the observations in Fig. 5, we can find out that four selected BESS technologies give similar results of RE installed capacities, approximately 17.2 and 39.4 GW, in 2025 and 2030, respectively, as shown in Fig. 5(a) and (b). However, some BESS technologies have more RE installed capacity than others in 2040. In Fig. 5(d), LAB requires additional 38.66 GW, 24.94 GW, and 46.74 GW RE installed capacities than LIB, NASB, and

VRFB in 2040, respectively. The crucial factor causing this difference is the efficiencies, maximum DOD, discharge time, and capital cost of ESS in each BESS technology. Among all six BESS technologies, LAB has the lowest maximum DOD, with a 60–70% value and a discharge time of up to 5 h. In addition, the LAB has the higher energy loss in the charging process within the four representative BESS technologies, directly increasing the required RE installed capacities for load balancing. Besides, from the observation, we can conclude that the variance of RE installed capacity by BESS technologies is conspicuous in high RE penetration but is minor in low RE penetration conditions. Though the high energy loss, low maximum DOD, and discharge time in BESS technologies cause the higher RE installed capacities and seems to foster the RE integration to a certain extent with higher RE installed capacities, those additional RE installed capacities actually result in enormous costs under the same climate goals. Therefore, since the objective of the OPF model is minimizing the total system cost in this study, the BESS technologies with less RE installed capacities are regarded as having better performance than the BESS technologies with higher RE installed capacities.

To further discuss the synergy between ESS and RE, the regional distributions of the generator's installed capacities are shown in Figs. 6 and 7. The tendency of the zonal RE installed capacities is similar among the BESS technologies. Therefore, we select the most popular BESS technology, LIB, as a demonstration to illustrate the spatial and temporal analysis of RE integration. The regional distributions of LIBs' generator installed capacities in 2025, 2030, 2035, and 2040 with different scenario settings are presented in Figs. 6 and 7. As shown in Fig. 6(a)-(d), 17.2, 39.8, 52.8, and 84.8 GW of RE sources are installed across NYS in 2025, 2030, 2035, and 2040 with high load projections, respectively. In between, zone A has a high RE installed capacity because it can provide the high local demand loads in zone A and its adjacent zones B and C.
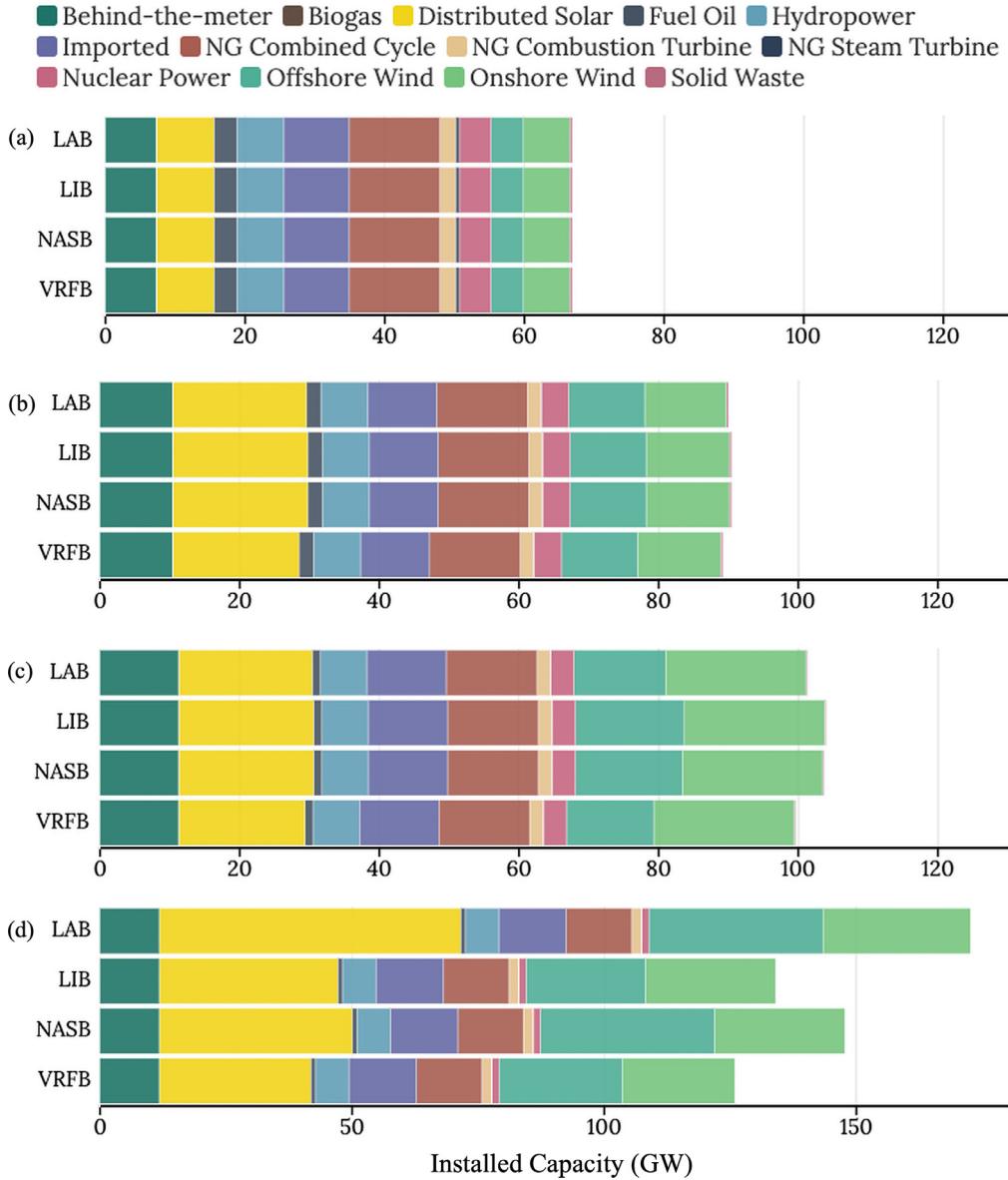
Fig. 5. The installed capacities of the four representative BESS technologies with high load projections in four representative years: (a) 2025, (b) 2030, (c) 2035, and (d) 2040.

Similarly, Zones F and G also have a high priority for RE installation because they are located near the heavily loaded center NYC. The trend of the preferred installation location for RE shows that the OPF model balances the energy production and loads within the minimum transmission distances. In addition, this trend of location preference for RE is also affected by the locations of the fossil-based generators, which are mainly near heavily loaded zones. The RE replaces the production of conventional generators because of the high RE penetration and energy transition requirements, causing the preferred installation location for RE to be closer to the heavily loaded zones.

To show the impact of load projection decrease on the RE installed capacity location preference, we select the high, medium, and low load projections with LIBs in the zero CO_2 emissions target in 2040 as the demonstration. The regional distributions of LIBs' generator installed capacities in 2040 with high, medium, and low load projections are shown in Fig. 6(d), Fig. 7(a), and (b), respectively. Zones B, C, J, and K are the zones that have significant reductions of RE installed capacities when the load projections decrease from high to low. The geographical selection priorities of RE installed capacities for zones B and C between

these zones are due to the unbalanced load distributions in NYS. NYC and its adjacent zones have the dominant demand loads. When the load decreases, zones B and C, which are far from NYC, have less installed capacity priority for RE, while the RE prefers to be installed near the heavily loaded zones. The reductions of RE installed capacity in zones J and K are mainly caused by the reduction of offshore wind power. In addition, it is worth noting that zone A, which is the farthest zone from NYC, supplies power to adjacent zones B and C. Therefore, the RE installed capacity in zone A decreases less than those in zones B and C, as shown in Fig. 7(a) and (b). From the discussion of Figs. 6 and 7, we can conclude that installing RE close to these heavily loaded zones makes the RE energy production possible to respond rapidly to the substantial demand loads. Moreover, ESS and RE's systematic and spatial synergies can significantly enhance the power system's reliability when responding to increasing loads and RE penetration. Considering that many worldwide power systems have unbalanced load distributions, our finding of the preferred installation locations for RE and ESS and their synergy for power system reliability enhancement shall also be applicable to other regional power systems. Future energy transition studies can ana-
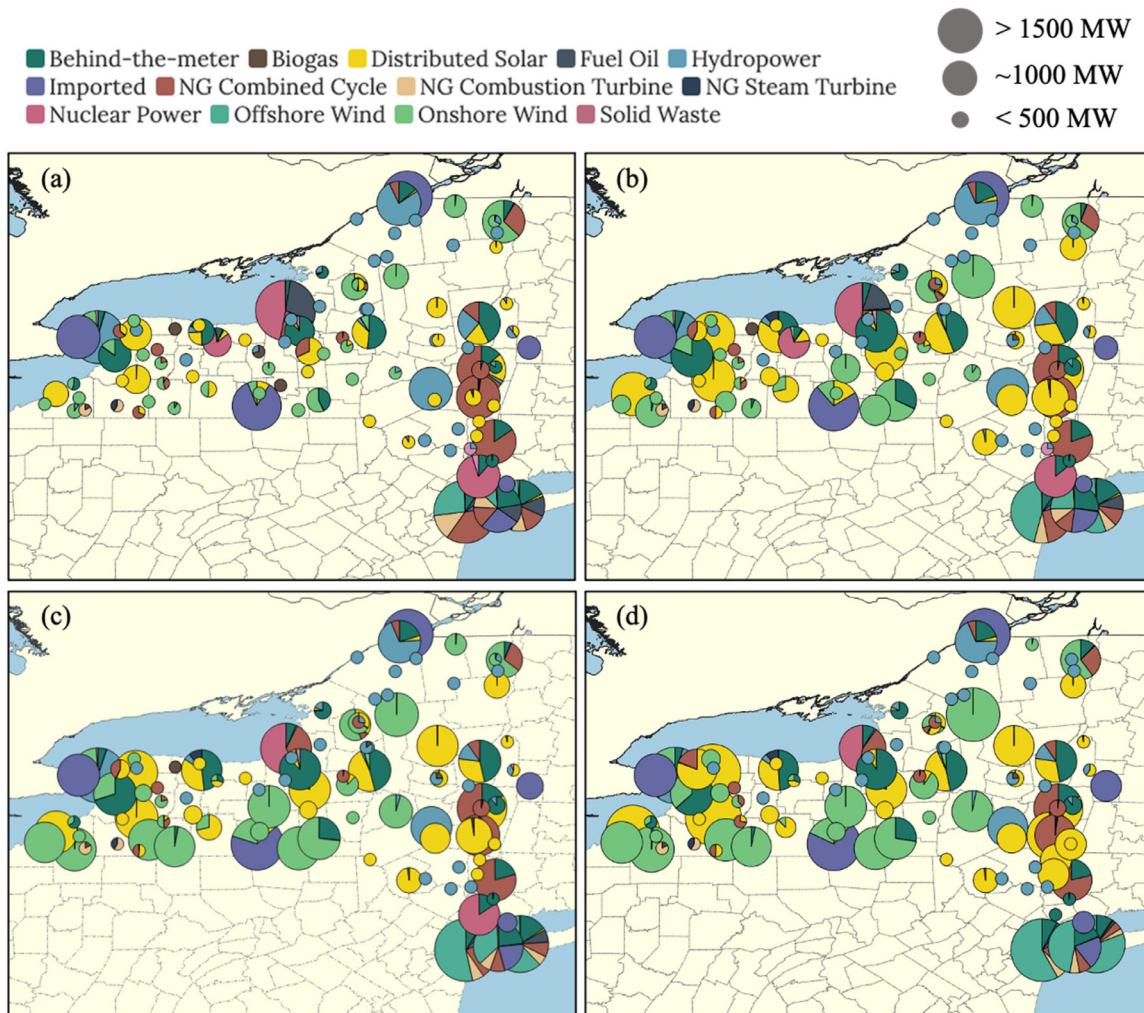
Fig. 6. The regional distributions of LIBs' generator installed capacity in the high load projection in the four representative years: (a) 2025, (b) 2030, (c) 2035, and (d) 2040.
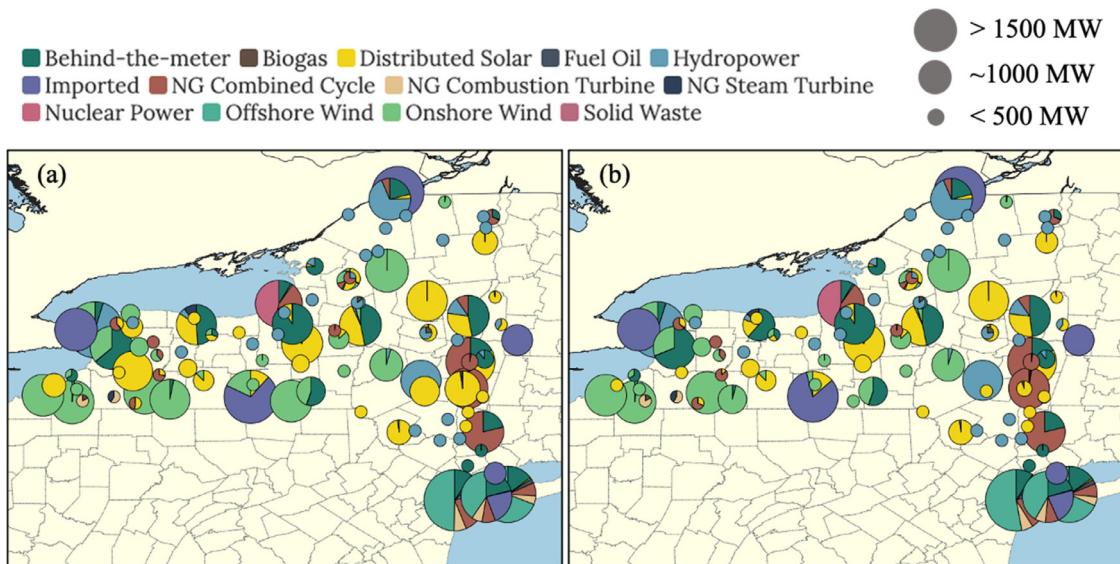
Fig. 7. The regional distributions of LIBs' generator installed capacity in 2040 with different load projections: (a) medium and (b) low.

lyze the synergy between having more RE installations near the heavily loaded areas and the additional grid-connected ESSs in the remote and lightly loaded areas to develop better systematic power system planning strategies and explore the potential improvement for the RE integration problem.

4.2. The impact of energy storage system technology on the power transmission system operation and carbon dioxide emissions

The bars in Fig. 4 give the zonal and total cycling numbers of different BESS technologies in the four representative years, 2025, 2030, 2035, and 2040. The increment of cycling numbers for BESS technologies is mainly caused by the increase of RE penetration in each representative year. The ESSs need a high cycling number to store the energy frequently from RE sources and dispatch the power frequently to meet the RE penetration increases, as shown in Fig. 4(a)-(d). The average cycling numbers of the four BESS technologies are approximately 500 times in 2025, 1100 times in 2030, 1300 times in 2035, and 1000 times in 2040. In addition, we can observe that zones B and C typically have greater cycling numbers due to their lightly loading conditions. Those zones are located far away from the load center of NYS and have the dispatch flexibility of transferring power from lightly loaded zones to heavily loaded zones [88]. In contrast, the heavily loaded zones, J and K, typically have slightly fewer cycling numbers because the power may be used locally to balance the high demand loads in NYC before being transmitted to the other zones.

In addition, we find a positive relationship between installed capacity and the cycling numbers of ESS. LIB typically has a low ESS installed capacity, resulting in lower cycling numbers in 2030 and 2035, as shown in Fig. 4(b) and (c). In contrast, LAB has large cycling numbers, approximately 1340 and 914 times in 2030 and 2040, respectively. In addition, among all BESS technologies, VRFB has the highest cycling numbers of 716, 1359, 1570, and 1151 in 2025, 2030, 2035, and 2040, respectively. It is because that VRFB has the highest discharge time, up to 12 h, allowing the ESS to operate at the rated power for a longer time compared to other BESS technology, such as LIB, with about up to 8 h of discharge time.

Moreover, Fig. 8 shows the ten cost terms in Eq. (1) with six BESS technologies and high load projections in 2025,2030, 2035, and 2040. The ten cost terms include the generator's capital, O&M, and retirement cost, ESS capital, O&M, replacement cost, line extension cost, and the CO_2 emissions social cost. It can be observed from Fig. 8(a)-(c) that the total generator capital costs of all the BESS technologies increase gradually by year from approximately \$30 billion to \$110 billion to satisfy the climate goals from 2025 to 2040. Besides, the total ESS capital costs increase significantly from 2025 to 2040 because more ESSs are installed to support high RE integration and achieve strict climate goals in optimized conditions. For instance, LIB has \$2.6, \$5.1, \$6.4, and \$22.4 billion of the ESS total capital costs in 2025, 2030, 2035, and 2040, respectively.

The results in Fig. 8 show that the highest social cost of CO_2 emissions occurs in 2025. The total CO_2 emissions social cost gradually decrease along the representative years 2025 to 2035 in Fig. 8(a)-(c) until it reaches zero CO_2 emissions in 2040. The significant reduction of CO_2 emissions social cost is caused by a 52% of CO_2 emissions decline between 2025 and 2030 and a 50% of CO_2 emissions decline between 2030 and 2035. When reviewing the crucial cost for the total system cost, we discover that the total ESS capital cost is the most critical cost among the BESS technologies between 2025 and 2040, as shown in Fig. 8(a)-(d). BESS technologies with a worse efficiency, a higher energy loss, low maximum DOD, or low discharge time, require additional RE and ESS installed capacities, which leads to higher total RE and ESS capital costs. For instance, NICDB, with the highest energy loss in the charging process, has an additional \$2.08 billion total system cost compared to LAB, the BESS technology having the lowest system cost in 2025, as shown in Fig. 8(a). Besides, as shown in Fig. 8(d),

the differences in total system cost by BESS technologies are significant in 2040, ranging from \$118 billion to \$173 billion, with a \$55 billion cost difference. These results illustrate that careful BESS technology selection is essential for cost-saving in power system planning with RE integration.

Also, BESS technologies with a shorter lifetime or a lower cycling limit require more frequent replacement. For instance, we observe that ZNBRB, NICDB, and LAB need to be replaced in 2030 due to reaching their short cycling limits of 2000, 3500, and 1800 cycles, which further leads to an increase in the capital cost, as shown in Fig. 8(b). Moreover, the zero CO_2 emissions target in 2040 will push more frequent ESS dispatches. Thus, due to cycling limits, LIB, NASB, NICDB, VRFB, ZNBRB, and LAB all need to be replaced in 2040. These replacements cause huge economic disadvantages for these BESS technologies. For instance, because NICDB requires replacements in 2030, NICDB requires an additional \$3.47 billion cost compared to the LIB in 2030. LIB requires replacement in 2035 and 2040, causing additional \$15.3 and \$54.5 billion costs compared to the VRFB. Therefore, we can conclude that BESS technologies with a low lifetime and a low cycling limit require more frequent replacement than other BESS technologies, leading to disadvantages for economic performance. Besides, the inevitable disadvantage of the technical performance for high energy loss ESS technologies directly affects the reliability of power system operation and results in higher system costs. These economic drawbacks become more significant when considering the longer analyzed horizon or reaching the zero CO_2 emissions target.

CO_2 emissions are important metrics to evaluate the energy transition progress. Therefore, we specifically discuss the CO_2 emissions of each BESS technology in each representative year. The operational CO_2 emissions of the generators with the six BESS technologies in 2025, 2030, and 2035 are presented in Fig. 9(a)-(c), respectively. The result of CO_2 emission in 2040 is not shown in Fig. 9 because the zero CO_2 emissions target will be achieved in 2040. As shown in Fig. 9(a)-(c), the six BESS technologies with high load projections have an average of 10.89, 5.23, and 2.61 million tons of CO_2 emissions in 2025, 2030, and 2035, respectively. In Fig. 9(b), the NICDB has 5.36, 4.17, and 3.70 million tons of CO_2 emissions in 2030 with high, medium, and low load projections, respectively. Those CO_2 emissions differences are caused by the different load projections, which can be referred to Table 2. Moreover, we find that the BESS technologies with a high energy loss rely more on fossil-based generators. For instance, as shown in Fig. 9(b), NICDB will cause higher CO_2 emissions in 2030, with values of 5.36, 4.17, and 3.70 million tons, than other BESS technologies. In contrast, VRFB, which have higher maximum DOD and discharge time, normally rely less on fossil-based generators and thus generate fewer CO_2 emissions of 5.05, 3.98, and 3.52 million tons in high, medium, and low load projection in 2030, respectively, as shown in Fig. 9(b). Similar tendencies of CO_2 emission for LIB, NASB, and LAB can also be found in 2035, with values of 2.51, 2.54, and 2.68 million tons of CO_2 emissions, as shown in Fig. 9(c). From the discussion of the CO_2 emissions differences among BESS technologies, we realize that the low maximum DOD and discharge time, and the unreliable power supply from the high energy loss BESS technologies cause additional CO_2 emissions. Because a huge amount of energy is wasted during the charging, discharging, and storing process, high energy loss BESS technologies require additional fossil-based generators' support to maintain reliable power supplies and balance the demand loads in the years before reaching the zero CO_2 emissions target. Thus, we can conclude that the BESS technologies with high energy losses, low maximum DOD, or low discharge time are less conducive to facilitating the energy transition than other BESS technologies due to their higher reliance on fossil-based generators.

Because the BESS technologies in our study perform differently for the installed capacities of RE, ESS, reliance on fossil-based generators, and the total system cost, the technical and economic characteristics of different ESS technologies should be fully clarified to prevent inaccurate ESS energy dispatch estimation and not hinder the evaluation of the
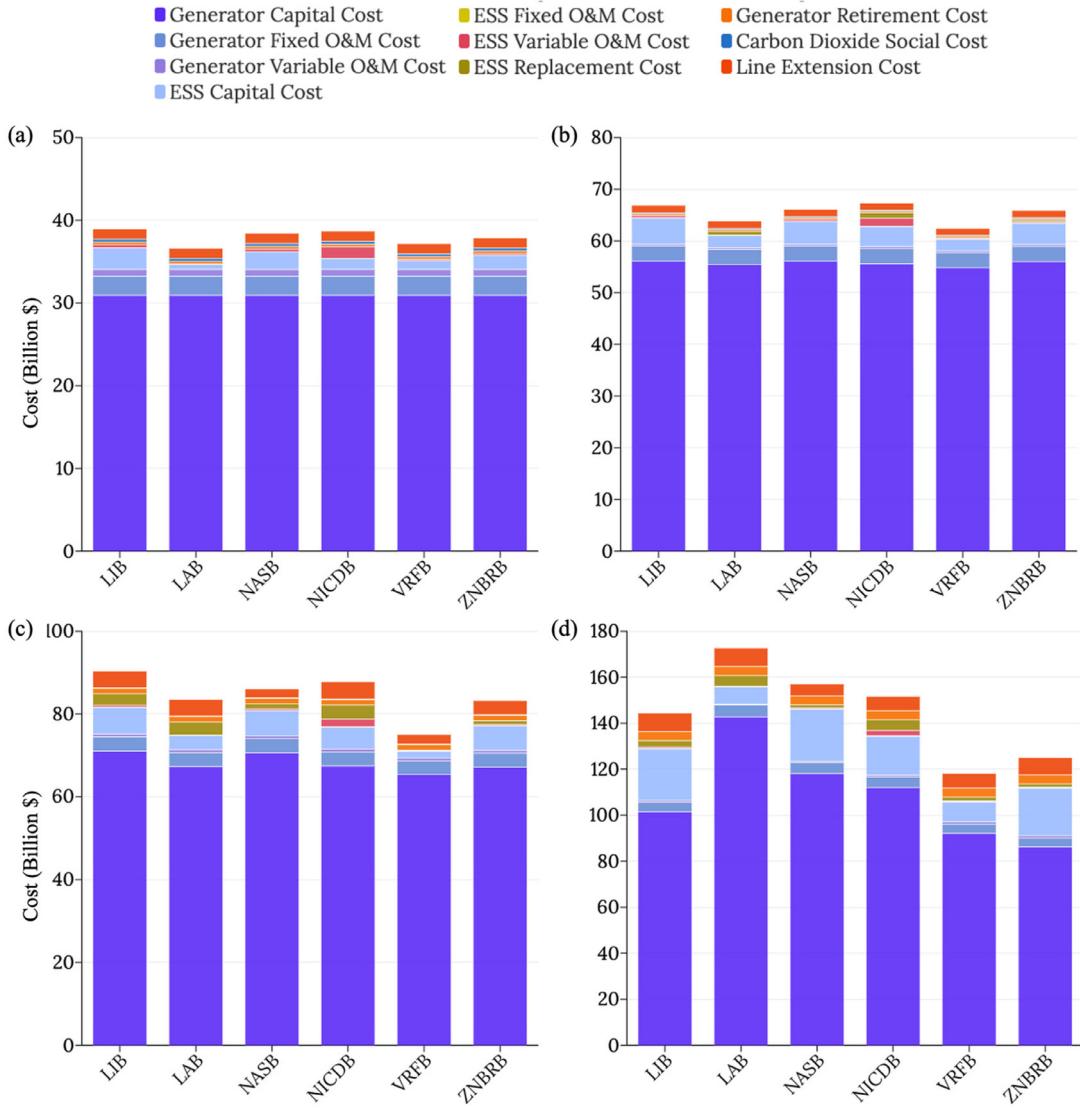
Fig. 8. The total system costs by ten cost categories for six BESS technologies in the high load projections in the four representative years: (a) 2025, (b) 2030, (c) 2035, and (d) 2040.

synergy between RE and ESS in the future power system and energy transition studies.

4.3. Multidimensional evaluation of the performance of energy storage system technology by scenario

Fig. 10 shows the cross-sensitivity analysis of the technical-economic ratios and PS-ESS ratios of six BESS technologies in the four representative years, 2025, 2030, and 2035. The y-axis is the PS-ESS ratio, which represents the percentage of focus on the power system operational performance or ESS performance. The x-axis is the technical-economic ratio, which represents the percentage of focus on technical or economic performance. The performance score can be significantly different when considering different criteria preferences. For example, in 2040, ZN-BRB has a 0.59 performance score in a 10% technical-economic ratio and a 90% PS-ESS ratio but only has a 0.24 performance score in a 90% technical-economic ratio and a 10% PS-ESS ratio. The performance scores of the BESS technologies are highly dependent upon the preferences for the technical, economic, and operational criteria.

When considering the discrepancies from the BESS technology perspective, NICDB has a worse performance than any of the BESS tech-

nologies in some representative years, which results in a range of performance scores from 0.1 to 0.3 in all the combinations of technical-economic and PS-ESS ratios. The main reason is that NICDB has the worst charge-discharge efficiencies with the highest O&M cost among all the BESS technologies. Besides, NICDB requires reinstallation, bringing the additional capital and replacement costs with economic disadvantage. Other BESS technologies, such as LIB, NASB, LAB, and ZNBRB, that require reinstallation between 2025 and 2035 usually have substantial economic disadvantages. However, LAB has a more negligible impact because its capital cost is lower than those of the other BESS technologies, with values of $450 per kW. Moreover, some BESS technologies will perform better in 2040. For instance, LAB has high performance scores only when having more preference for economic criteria. VRFB has a high score ranging mostly from 0.60 to 0.72 due to its low capital cost, high cycling limits, and longest discharge time compared to other BESS technologies.

Moreover, some BESS technologies perform better in specific representative years or criteria preferences. For instance, NASB and VRFB have stable technical, economic, and operational performances, with high performance scores of approximately 0.79 and 0.65 in 2025, respectively. However, some BESS technologies have worse performance
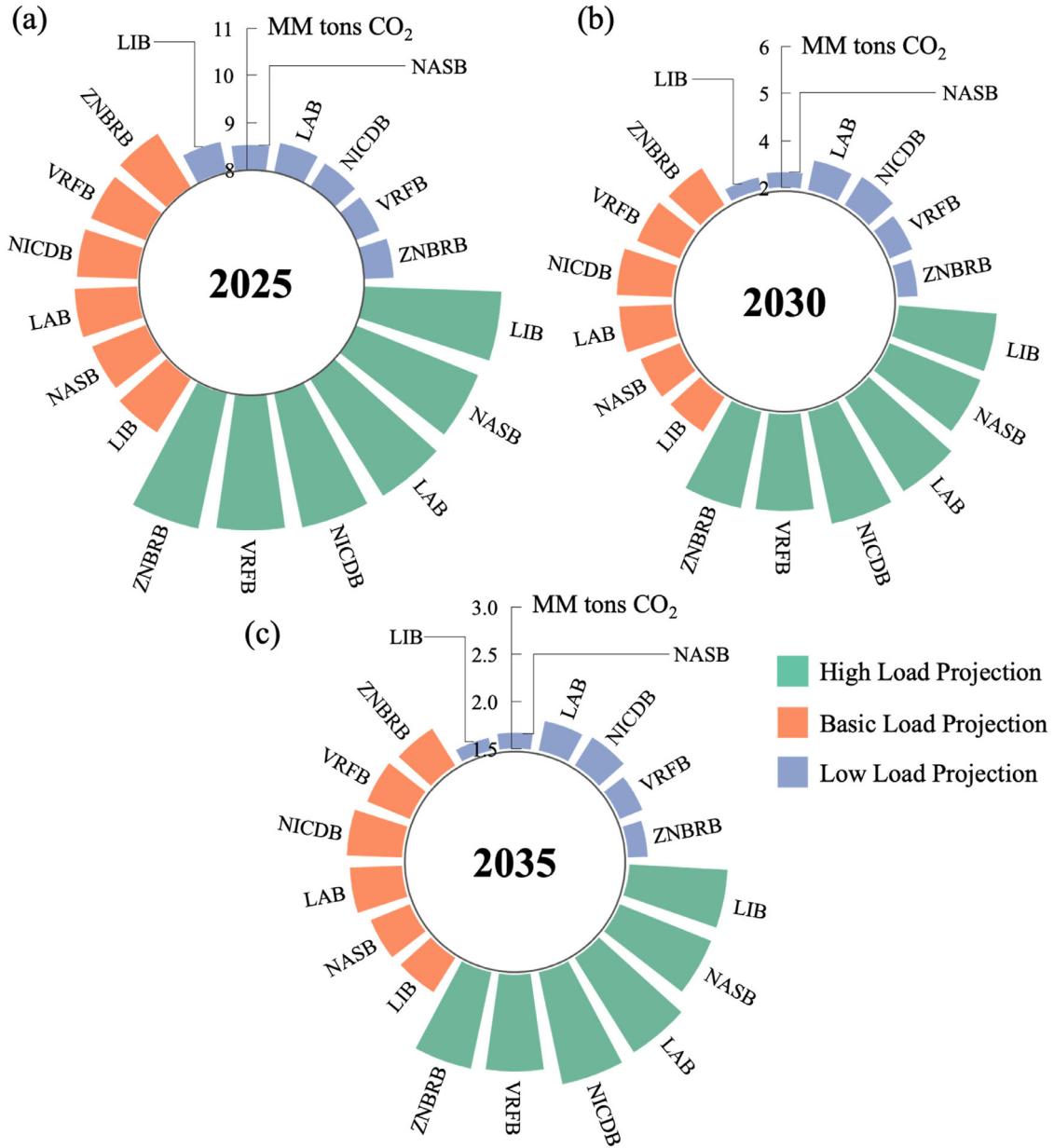
Fig. 9. The CO_2 emissions in power system operation with six BESS technologies in the high, medium, and low load projections in three representative years: (a) 2025, (b) 2030, and (c) 2035.

starting from specific years than others. For instance, the BESS technologies with either a high capital cost or a high replacement cost, such as LIB and NASB, with the original average capital costs of $2600 per kW and $2000 per kW, have difficulty compensating for the economic drawbacks. Even though LIB has the highest specific power, specific energy, and energy density, the higher technical performance cannot greatly mitigate the economic disadvantage. Thus, LIB usually has performance scores mostly between 0.35 and 0.5 when economic criteria are preferred.

We also review the performance scores of six BESS technologies in 2040, the target year of reaching zero carbon emissions. The ranking of the BESS technologies follows the sequence of VRFB, LAB, NASB, LIB, ZNBRB, and NICDB with average performance scores of 0.546, 0.514, 0.491, 0.487, 0.485, 0.387 in all combinations of ratios, respectively. VRFB obtains the highest performance score because of its high cycling limit, low capital cost, high maximum DOD, and high discharge time compared to other BESS technologies. In contrast, NICDB obtains the

lowest performance score because of worse operational performance and high energy loss. However, The BESS technology selection should be flexible and can be determined by the preference of the criteria or scenarios considering the different BESS technologies perform differently by criteria. When having greater consideration of the technical criteria, LIB and NASB are better choices than the others because of their combined performances based on their specific power, energy density, and efficiencies. With greater consideration of the economic criteria, LAB and VRFB are the BESS technologies with outstanding performance due to the low capital costs. Moreover, when having greater consideration of the operational criteria, NASB and VRFB are the better options among all of the ESS technologies since they have better synergies with the power system by having high cycling and discharge efficiency with low energy loss.

Compared to our results of the BESS technology selection presented in Section 4.3, many previous MCDM studies [44] have mentioned that LIB has the highest selection priority for power systems or grid-related
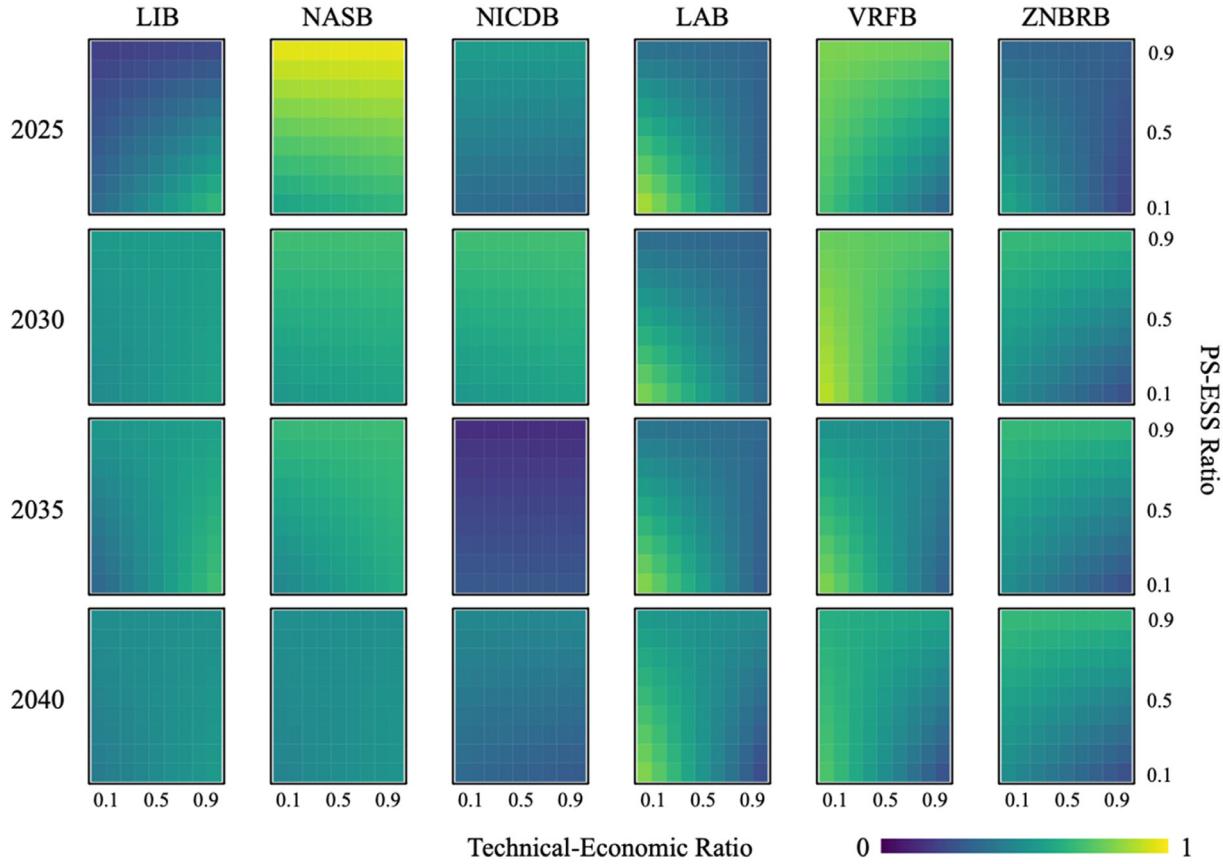
Fig. 10. The performance scores of the six BESS technologies in the four representative years are based on the cross-sensitively analysis of the technical-economic and PS-ESS ratios.

applications. The main reason is that they usually consider the social criteria impact, such as social acceptance [89]. The market and consumer generally have a high confidence score for LIB, leading to high performance on social criteria. In addition, if an evaluation does not include the power system's operational performance and RE integration target, it will not cover the reinstallation costs. Considering that the lifetime of the common LIBs is ten years, and the cycling limit is 2250 times, it has a great chance to be reinstalled in the power system frequently when in high RE penetration conditions that requires frequent dispatches from the ESS to mitigate intermittent power supplies from RE. Therefore, LIB's overall performance may not be as optimistic as that determined by the evaluations based only on its inherent characteristics without the power system operation involved. In contrast, VRFB received an average performance rating in the previous MCDM studies because it is still under development. However, VRFB has expected more technical improvement in the next decades. Although VRFB's inherent economic and technical performances are not the best, high maximum DOD, long discharge time, and high cycling limit give it certain advantages, especially when the analyzing horizon of RE integration is long. We can expect a more mature grid-scale application for VRFB in the near future (Fig. 10).

5. Conclusions

In this study, an integrated optimal power flow-multiple-criteria decision-making model with extensive future scenarios was proposed to investigate six battery energy storage system technologies' impact on the power transmission system operation with renewable energy integration to satisfy the New York State stage-wise climate goals from 2025 to 2040. The extensive future scenario design considered the future de-

velopments of battery energy storage system technologies and generators, policy restriction of carbon dioxide emissions, load projections, and climate goals. The proposed method could identify the most critical features of battery energy storage system technologies to enhance renewable energy integration and achieve New York State's climate goals.

Based on the spatial and temporal analysis, we concluded that the preferred installed locations of the energy storage system and renewable energy were highly correlated with the load distributions. The synergy between the energy storage system and renewable energy was crucial to enhance the reliability of power system operation, especially when the zero carbon dioxide emission target is achieved in 2040. The synergy between the energy storage system and renewable energy could also help future renewable energy integration studies analyze the benefits of integrating renewable energy in power systems with energy storage systems. When comparing the performance of different battery energy storage system technologies, we discovered that technologies with high energy loss, low maximum depth of discharge, and low discharge time could reduce the reliability of power system operation. They required additional power supplies than other battery energy storage system technologies to satisfy climate goals. For example, the lead-acid battery, with the high energy loss, low maximum depth of discharge, and low discharge time among six battery energy storage technologies, required an additional 38.66 GW renewable energy capacity than the lithium-ion battery in 2040 and generated 2.9% additional carbon dioxide emissions than the lithium-ion battery on average. In addition, the energy storage system technologies with short lifetimes and cycling limits required frequent replacement, especially when analyzing high renewable energy integration targets in the long horizon. Therefore, we raised two suggestions on energy storage system configurations in power systems and energy transition studies. The first suggestion was that energy storage system tech-

nologies' technical and economic characteristics should be thoroughly clarified to avoid inaccurate estimation of energy storage systems' power dispatches. The second suggestion was that the system planner should carefully review some characteristics of the energy storage system technologies and their impacts on the reliability of power system operation, such as the energy storage system technologies with high energy loss and low energy loss. Furthermore, based on the cross-sensitively analysis of the technical, economic, and operational criteria, we found that the vanadium redox flow battery had the highest performance score, with an average score of 0.546 in 2040, because of its high cycling limits, high maximum depth of discharge, and long discharge time. In contrast, the nickel-cadmium battery had the lowest score in 2040, with an average score of 0.387, due to its high energy loss, low cycling limit, and high capital cost. The lithium-ion, lead-acid, and sodium-sulfur battery had the top selection priority when the technical, economic, and operational criteria were preferred, respectively.

Declaration of Competing Interest

The authors declare that they have no known competing financial interests or personal relationships that could have appeared to influence the work reported in this paper.

Data availability

Data will be made available on request.

Appendix A: Energy storage system technology selection, characteristics review, and future cost simulation

Appendix A presents the process of ESS technology selection, characteristics review, and future cost reduction simulation as the first step mentioned in the research framework in Section 3.1 and as shown in Fig. 1. Based on the literature reviews of several current ESS technology developments [90] and prospects reviews [51] and assessments [91] from different domains in power and energy systems [92], such as versatile applications [46], distribution networks [93], sizing and control [94], smart girds [95], microgrids [96], and ESS roles and impact [97] in large scale RE integration [57], we select six typical ESS technologies and the reasons why the ESS technology is selected are summarized in Table A.1. Specifically, in our study, the ESS technology shall be scalable and used for large-scale energy management in the power system. Hence, the ESS technologies used in our study can further be classified as the battery energy storage system (BESS). In addition, it is worth noting that our study does not consider pumped hydrogen storage (PHS), one of the common ESS technologies [98] but has less flexibility since its construction and implementation is restricted by geographical conditions [76]. Its extension is not planned by NYISO in NYS's gold book [60] and the power trend report [48], and its capacity cannot be scalable easily. The economic and technical characteristics of the six BESS technologies collected from previous ESS review studies are summarized in Tables A.2 and A.3.

Table A.1
The consideration of ESS technology choices is based on the development, implementation, and suitability for the large-scale energy management of the case study.

ESS technology	Selection	Reasons for selection
Lithium–ion battery (LIB)	Yes	The LIB is the most commonly used technology in studies and applications in power systems [10] and electric vehicles (EVs) [99]. It obtains the most focus in future implementation and can be potentially used for energy management [57].
Sodium–sulfur battery (NASB)	Yes	This ESS technology has been utilized in RE integration [100] and evaluation processes [79] in the energy transition problem. The high specific energy makes NASB more easily scalable for the implementation of RE integration [57].
Lead–acid battery (LAB)	Yes	Although there is concern about pollution in the recycling process, some studies have pointed out that the environmental impact can be mitigated by the advance recycle method with an improved technique [101]. Hence, it is still a preferred ESS technology for optimization [102] and assessment [103] studies of power systems.
Hydrogen energy storage (HES)	No	This technology is the focused investment and development target in the NYS power system [104] and future grid design [105]. However, HES is still in the early developing stage [106] and is not scalable and not applicable for large-scale applications, considering the chemical process requires expensive catalysts and restricted storage conditions for the hydrogen [51].
Superconducting magnetic energy storage (SMES)	No	This advanced ESS technology has a low capital cost, long lifetime, and high energy density making it able to stabilize the intermittent RE supply [107] and support the power system's energy transition [57]. However, SMES typically used for voltage regulation [52] and does not apply to large-scale applications.
Supercapacitor energy storage (SCES)	No	This advanced ESS technology has bullish prospects due to its low capital cost, long lifetime, and high energy density, which allow it to smooth the voltage of the RE power supply [108] in future power systems [97], but not applicable for energy management in large-scale applications.
Nickel–cadmium battery (NICDB)	Yes	This mature ESS technology has been used in ESS technology selection studies [44] and grid-level and large-scale power system studies [109].
Vanadium redox flow battery (VRFB)	Yes	The most developed flow battery. It is expected to have additional technical innovations and price reductions [110] with competitive development [96].
Flywheel energy storage (FES)	No	This mature mechanical ESS is typically used for applications and studies in the power system [111] or EV power supply [11]. However, the short discharge time and the high self-discharge ratio make FES only applicable for short-term applications [51].
Underground compressed air energy storage (CAES)	No	This mature and classic mechanical energy storage system has been used in large-scale power systems [112] and studied in power system optimization problems [113]. However, CAES scalability is based on the suitability of geological formations for gas vessel construction, which cannot be scalable easily [51].
Pumped Hydrogen Storage (PHS)	No	The ESS technology has the largest installed capacity for grid-connected applications [46]. However, constructing PHS requires geographical availability, such as the high altitude between revivors, which cannot be scalable and thus not be considered.
Zinc–bromine battery (ZNBRB)	Yes	The classic flow battery has a high discharge time, high energy density, and deep depth of discharge [46]. The advantage makes ZNBRB can be potentially used for large-scale applications.
Polysulfide bromine flow battery (PSB)	No	The typical flow battery has a quick response time but low efficiency. In addition, PSB is still under development for technology improvement and has no experience in large-scale applications and commercial operations [46]. Therefore, PSB is not considered in our study.
Thermal chemical heat storage (TCES)	No	Some mature TECS technologies require specific preservation and are not allowed to freeze, which is unsuitable for NYS weather conditions. The other TECS technologies need the improvement of storage medium to increase the extendability[57]. Hence, TCES is not considered in this study.

Table A.2

The main economic characteristics of BESS technologies used in our study.

Technology	Capital cost ($/kW)	Fixed O&M cost ($/kW-yr)	Variable O&M cost ($/MWh)	Replacement Cost ($/kW)
LIB	1200–4000 [46]	2.2–15.2 [53]	0.44–6.22 [53]	207.6–602.7 [53]
NASB	1000–3000 [46]	2.2–19.2 [53]	0.33–6.22 [53]	199.8–491.7 [53]
LAB	300–600 [46]	3.6–14.4 [53]	0.17–0.58 [53]	55.5–621.6 [53]
NICDB	500–1500 [46]	4.4–26.6 [53]	8.81 [56]	530.6–636.0 [53]
VRFB	600–1500 [46]	3.8–19.2 [53]	0.22–3.11 [53]	123.2–213.1 [53]
ZNBRB	400–2500 [46]	3.6–7.7 [53]	0.33–2.22 [53]	112.1–223.1 [53]

Table A.3

The main technical characteristics of the BESS technologies used in our study.

Technology	Lifetime (years)	Cycling Limit	Cycling efficiency (%)	Discharge efficiency (%)	Maximum DOD (%)	Discharge time at rated power (h)	Self-discharge rate (%/day)
LIB	5–15 [46]	1500–3500 [51]	90–97 [52]	85 [52]	80 [115]	1–8 [52]	0.1–0.3 [46]
NASB	15–20 [46]	2500–4500 [52]	75–90 [52]	85 [52]	90 [115]	4–8 [91]	0.05 [46]
LAB	5–15 [46]	200–1800 [52]	63–90 [52]	85 [52]	60-70 [115]	1–5 [91]	<0.1 [46]
NICDB	10–20 [46]	3500 [51]	60–83 [52]	85 [52]	100 [115]	6–8 [91]	0.2–0.6 [46]
VRFB	5–20 [46]	12,000+ [52]	75–85 [52]	75–82 [52]	100 [115]	2–12 [91]	0.15 [46]
ZNBRB	5–20 [46]	2000+ [52]	66–80 [52]	66–70 [52]	100 [115]	1–10 [52]	Almost 0 [46]

From the review of the BESS technology characteristics, we discover that it is difficult to conclude which BESS technology performs better by comparing single characteristics without systematically analyzing multiple characteristics using the integrated OPF-MCDM model. For instance, NICDB has high O&M and replacement costs but a relatively low capital cost with an average lifetime among all BESS technologies. Therefore, a systematical and multidimensional evaluation is required, and we can eventually obtain the BESS technologies' performance scores by importing all the parameters from the tables into the integrated OPF-MCDM model. In addition, we can have a relatively fair mechanism to compare and select ESS technology for RE integration and energy transition.

In addition, because the time span of our study is relatively long, from 2025 to 2040, future cost reductions of ESSs may occur due to the optimization of installation and component manufacturing [114]. Hence, we adopt the concept of ESS technology cost prediction from the NREL [64]: using conservative, moderate, and advanced technology innovation scenarios with three different decline ratios to simulate future ESS technology cost reductions. From the above reviews of BESS technologies, if more than half of the studies point out promising prospects for developing ESS technologies (LIB, VRFB), the BESS technologies are partitioned into advanced innovation scenarios. If the BESS technologies (LAB and NICDB) receive few notices or have environmental concerns, they are partitioned into conservative innovation scenarios. The other BESS technologies (NASB and ZNBRB) receive mixed opinions on future growth and are partitioned into moderate innovation scenarios. The various cost decline ratios by innovation scenario are attached to all the BESS technology costs when reaching a specific year in the integrated OPF-MCDM model.

Appendix B: Constraints of the optimal power flow model

Appendix B describes the four types of constraints utilized in our OPF model, including generator constraints, ESS constraints, network operational constraints, and the annual CO$_2$ emissions and RE production constraints presented in Sections B.1, B.2, B.3, and B.4, respectively. The objective function of the OPF model is presented in Section 3.2.

Generator constraints

The generator constraints restrict the locational generator's power dispatch, capacity extension, and retirement year. First, the generator dispatch $P_{ss,b,r,t}^{G}$ at bus b with energy carrier r at time t in the scenario ss is constrained by its installed capacity $M_{ss,b,r}^{G}$, as shown in Eq. (B1).

$$0 \leq P_{ss,b,r,t}^{G} \leq M_{ss,b,r}^{G} \cdot \overline{g}_{b,r,t} \cdot X_{y,b,r}^{G}, \forall ss \in SS, \forall y \in Y, \forall b \in B, \forall r \in R, \forall t \in T \quad \text{(B1)}$$

where B is the set of buses in the model, R is the set of energy carriers, and T is the set of hours within a year. $\overline{g}_{b,r,t}$ is the time-dependent availability. The values of the availability $\overline{g}_{b,r,t}$ of RE sources, such as onshore wind power, offshore wind power, and distributed solar, are determined by weather conditions and radiation intensity obtained from the NREL integrated dataset toolkit [116]. For the other generator carriers, the values of their availability $\overline{g}_{b,r,t}$ are defined as their maximum operation thresholds, which are usually constant. The generator installed capacity $M_{ss,b,r}^{G}$ values are composited by the installed capacities from existing facilities $M_{ss,b,r}^{EX}$ and the extendable RE installation $M_{ss,b,r}^{RE}$. Considering current studies have concentrated on the dispatchable RE [68], mentioning the dispatch ability of RE is crucial for future power system design [70] and the dispatch ability of RE can be improved by algorithms [69] or energy management systems (EMSs) [66]. We assume all energy carriers are dispatchable in our optimization framework. In addition, for the retirement evaluation, $X_{y,b,r}^{G}$ is the generator retirement indicator, which is a binary variable considering the safe operation of generators. In the case where the difference between year y and the in-service date y_{is} is larger than the generator's lifetime y_{lmt}, $X^{G}=0$; otherwise, $X^{G}=1$, meaning the generator is still in service in year y, as denoted in Eq. (B2).

$$\begin{cases} X_{y,b,r}^{G} = 1 \text{ if } y - y_{is} \leq y_{lmt} \\ X_{y,b,r}^{G} = 0 \text{ else} \end{cases}, \forall y \in Y, \forall b \in B, \forall r \in R \quad \text{(B2)}$$

For generator capacity extensions, the installed capacity $M_{ss,b,r}^{RE}$ is constrained by the extension threshold $H_{y,b,r}^{RE}$ and the capacity from the previous year, as shown in Eq. (B3). In this study, one of the main focuses on generators is RE integration in future power systems. Thus, only RE is extendable, and r belongs to the RE subset R_{RE}.

$$M_{e,s,y-1,b,r}^{RE} \leq M_{ss,b,r}^{RE} \leq H_{y,b,r}^{RE}, \forall ss \in SS, \forall e \in E, \forall s \in S, \forall y \in Y, \forall b \in B, \forall r \in R_{RE} \quad \text{(B3)}$$

In addition, Eqs. (B4)–(B7) calculate the annual generator capital cost, annual generator fixed O&M cost and variable O&M cost, and generator retirement cost, respectively.

$$C_{ss}^{GC} = \sum_{b \in B} \sum_{r \in RE} (M_{ss,b,r}^{RE} - M_{e,s,y-1,b,r}^{RE}) \cdot c_{y,r}^{GC}, \forall ss \in SS, \forall e \in E, \forall s \in S, \forall y \in Y \quad \text{(B4)}$$

$$C_{ss}^{GF} = \sum_{b \in B} \sum_{r \in R} M_{ss,b,r}^{G} \cdot c_{y,r}^{GF}, \forall ss \in SS, \forall y \in Y \quad \text{(B5)}$$

$$C_{ss}^{GV} = \sum_{t \in T} \sum_{b \in B} \sum_{r \in R} P_{ss,b,r,t}^{G} \cdot (c_{y,r}^{GV} + D_r \cdot c_y^d), \forall ss \in SS, \forall y \in Y \quad \text{(B6)}$$

$$C_{ss}^{GR} = \sum_{b \in B} \sum_{r \in R} M_{ss,b,r}^{G} \cdot (1 - X_{y,b,r}^{G}) \cdot c_{y,r}^{GR}, \forall s \in SS, \forall y \in Y \qquad (B7)$$

where $c_{y,r}^{GC}$ is the generator unit capital cost, $c_{y,r}^{GF}$ is the annual generator unit fixed O&M cost, $c_{y,r}^{GV}$ is the hourly generator unit variable O&M cost, and $c_{y,r}^{GR}$ is the unit retirement cost for generator carrier r in year y. D_r and e_y^d are the unit emission of generator carrier r and the emissions social cost of CO_2 in year y, from the investigations of the previous studies [65].

Energy storage system constraints

The dispatch $P_{ss,b,t}^{ESS}$ of the ESS at bus b with the technology e at time t in the ss scenario is constrained by the installed capacity of the ESS $M_{ss,b}^{ESS}$, as shown in Eq. (B8).

$$z \cdot \eta_e^{cyc} \cdot M_{ss,b}^{ESS} \leq P_{ss,b,t}^{ESS} \leq z \cdot \eta_e^{disc} \cdot M_{ss,b}^{ESS}, \forall ss \in SS, \forall b \in B, \forall t \in T \qquad (B8)$$

where z is a binary variable indicating whether the ESS is charging or discharging. η_e^{cyc} is the round-trip, or so-called cycling efficiency, and η_e^{disc} is the discharge efficiency. In addition, the relationship for the energy level $EL_{ss,b,t}$ in ESS between time t and the previous hour $t-1$ can be represented as Eq. (B9).

$$EL_{ss,b,t} = EL_{ss,b,t-1} - \triangle t \times P_{ss,b,t}^{ESS} - \frac{\eta_e^{self}}{24}, \forall ss \in SS, \forall e \in E, \forall b \in B, \forall t \in T \qquad (B9)$$

where η_e^{self} is the daily self-discharge ratio of ESS technology e. $\triangle t$ represents the hourly time resolution in our model. $EL_{ss,b,t}$ is the energy level in the ESS at bus b and time t. Furthermore, for the ESS capacity extensions, the installed capacity $M_{ss,b}^{ESS}$ at bus b in the ss scenario and year y is constrained by the ESS capacity extension threshold $H_{y,b}^{ESS}$, and the capacity installed in the previous year, as shown in Eq. (B10).

$$M_{e,s,y-1,b}^{ESS} \leq M_{ss,b}^{ESS} \leq H_{y,b}^{ESS}, \forall ss \in SS, \forall e \in E, \forall s \in S, \forall y \in Y, \forall b \in B \qquad (B10)$$

and Eq. (B11) evaluates whether the ESS needs to be replaced in year y by the indicator $X_{e,y,b}^{ESS}$. We assume the ESS in-service date is in 2025 and assume that the annual cycling of each ESS technology is increased by the load increment ratio by years between the representative years to evaluate the replacements.

$$\begin{cases} X_{e,y,b}^{ESS} = 1 \, if \, y - y_{eis} \geq y_{elt} \\ X_{e,y,b}^{ESS} = 1 \, if \, N_e \geq N_e^{lmt} \\ X_{e,y,b}^{ESS} = 0 \, else \end{cases}, \forall e \in E, \forall y \in Y, \forall b \in B \qquad (B11)$$

If the ESS system's in-service year y_{eis} and year y difference are more than the ESS technology lifetime y_{elt}, or the accumulated cycling time N_e is larger or equal to the cycling limit N_e^{lmt}, the indicator $X_{e,y,b}^{ESS} = 1$; otherwise, $X_{e,y,b}^{ESS} = 0$. In addition, the annual ESS capital cost, annual ESS fixed O&M cost, annual ESS variable O&M cost, and the replacement cost of ESS are denoted in Eqs. (B12), (B13), (B14), and (B15), respectively.

$$C_{ss}^{EC} = (\sum_{b \in B} (M_{ss,b}^{ESS} - M_{e,s,y-1,b}^{ESS}) + \sum_{b \in B} M_{e,s,y-1,b}^{ESS} \cdot X_{e,y,b}^{ESS}) \cdot c_{e,y}^{EC}, \\ \forall ss \in SS, \forall e \in E, \forall s \in S, \forall y \in Y, \forall b \in B \qquad (B12)$$

$$C_{ss}^{EF} = \sum_{b \in B} M_{ss,b}^{ESS} \cdot c_{e,y}^{EF}, \forall ss \in SS, \forall e \in E, \forall y \in Y \qquad (B13)$$

$$C_{ss}^{EV} = \sum_{t \in T} \sum_{b \in B} P_{ss,b,t}^{ESS} \cdot c_{e,y}^{EV}, \forall ss \in SS, \forall e \in E, \forall y \in Y \qquad (B14)$$

$$C_{ss}^{ER} = \sum_{b \in B} M_{ss,b}^{ESS} \cdot X_{e,y,b}^{ESS} \cdot c_{e,y}^{ER}, \forall ss \in SS, \forall e \in E, \forall y \in Y \qquad (B15)$$

where $c_{e,y}^{EC}$ is the ESS unit capital cost, $c_{e,y}^{EF}$ is the ESS unit fixed O&M cost, $c_{e,y}^{EV}$ is the hourly ESS unit variable O&M cost, and $c_{e,y}^{ER}$ is the unit replacement cost for ESS in year y.

Network operational constraints

The power demand $P_{ss,b,t}^{LD}$ at bus b at time t in scenario ss in year y is balanced by either the generators or ESS discharge at bus b or the dispatch from other buses through branch l with the power flow, as shown in Eqs. (B16), (B17), and (B18), respectively.

$$\sum_r P_{ss,b,r,t}^{G} + P_{ss,b,t}^{ESS} - P_{ss,b,t}^{LD} = \sum_l P_{ss,l,t}^{F}, \forall ss \in SS, \forall b \in B, \forall t \in T \qquad (B16)$$

$$P_{ss,l,t}^{F} = BB_{ij}(\theta_{i,t} - \theta_{j,t}) \forall ss \in SS, \forall t \in T, \forall l \in L, \forall i \in B, \forall j \in B \qquad (B17)$$

$$\theta_1 = 0 \qquad (B18)$$

where $P_{ss,b,r,t}^{G}$ is the generator dispatch at bus b with carrier r at time t in scenario ss, $P_{ss,b,t}^{ESS}$ is the ESS dispatch at bus b and in time t in scenario ss, and $P_{ss,l,t}^{F}$ is the power flow from transmission line l connected to bus i and j at time t in scenario ss. The power flow $P_{ss,l,t}^{F}$ is equal to the product of the susceptance BB_{ij} of the transmission line and the voltage phase angle θ_j difference between buses i and j at time t. The slack bus voltage phase angles θ_1 are settled to 0. In addition, the amounts of power flow are constrained by the apparent power $M_{ss,i,j}^{AP}$, as given in Eq. (B19). i and j are the buses connected by transmission line l. Negative and positive power flow represents the flow direction between buses i and j.

$$-M_{ss,i,j}^{AP} \leq BB_{ij}(\theta_i - \theta_j) \leq M_{ss,i,j}^{AP}, \forall ss \in SS, \forall i \in B, \forall j \in B \qquad (B19)$$

For the line capacity extensions, the apparent power $M_{ss,l}^{AP}$ at branch l in the ss scenario and year y is optimized between the original values and the maximum extended factor α_l, as shown in Eq. (B20).

$$M_{ss,l}^{AP} \leq M_l^{AP} \cdot \alpha_l, \forall s \in SS, \forall l \in L \qquad (B20)$$

Annual carbon dioxide emissions and RE production constraints

Energy production and CO_2 emissions constraints are from the stage-wide climate goals mentioned in Section 3.2, including CO_2 emissions and RE production. The CO_2 emissions are caused by the generator operation. The expression is described in Eq. (B21).

$$\sum_{b \in B} \sum_{r \in R} \sum_{t \in T} P_{ss,b,r,t}^{G} \cdot \overline{g}_{b,r,t} \cdot D_r \leq CEL_y, \forall ss \in SS, \forall y \in Y \qquad (B21)$$

where $P_{ss,b,r,t}^{G}$ is the energy dispatch from generators, $\overline{g}_{b,r,t}$ is the availably or maximum output of the generators, and D_r is the unit emission of the generator carrier r. The total CO_2 emissions shall be less than or equal to the year's emission target CEL_y. On the other hand, the RE production constraints force the RE dispatch to reach the expectation of stage-wise climate goals [69] toward energy transition in NYS, as shown in Eq. (B22).

$$\sum_{b \in B} \sum_{r \in R_{RE}} \sum_{t \in T} P_{ss,b,r,t}^{G} \cdot \overline{g}_{b,r,t} \geq \sum_{b,t} P_{ss,b,t}^{LD} \cdot RP_{y,r}, \forall ss \in SS, \forall y \in Y, \forall r \in R_{RE} \qquad (B22)$$

where $P_{ss,b,r,t}^{G}$ is the generator power dispatch, $\overline{g}_{b,r,t}$ is the availability of RE at time t, $P_{ss,b,t}^{LD}$ is the load at bus b at time t in scenario ss, and $RP_{y,r}$ is the RE penetration target ratio in year y.

References

[1] Kober T, Schiffer HW, Densing M, Panos E. Global energy perspectives to 2060–WEC's World Energy Scenarios 2019. Energy Strateg Rev 2020;31:100523.

[2] Rogelj J, Den Elzen M, Höhne N, Fransen T, Fekete H, Winkler H, et al. Paris Agreement climate proposals need a boost to keep warming well below 2 C. Nature 2016;534:631–9.

[3] Liu L, Wang Z, Wang Y, Wang J, Chang R, He G, et al. Optimizing wind/solar combinations at finer scales to mitigate renewable energy variability in China. Renew Sustain Energy Rev 2020;132:110151.

[4] Liang X. Emerging power quality challenges due to integration of renewable energy sources. IEEE Trans Ind Appl 2016;53:855–66.

[5] Sinsel SR, Riemke RL, Hoffmann VH. Challenges and solution technologies for the integration of variable renewable energy sources—A review. Renew Energy 2020;145:2271–85.

[6] Zhao H, Wu Q, Hu S, Xu H, Rasmussen CN. Review of energy storage system for wind power integration support. Appl Energy 2015;137:545–53.

[7] Kalair A, Abas N, Saleem MS, Kalair AR, Khan N. Role of energy storage systems in energy transition from fossil fuels to renewables. Energy Storage 2021;3:e135.

[8] Cebulla F, Haas J, Eichman J, Nowak W, Mancarella P. How much electrical energy storage do we need? A synthesis for the US, Europe, and Germany. J Clean Prod 2018;181:449–59.

[9] Cárdenas B, Swinfen-Styles L, Rouse J, Hoskin A, Xu W, Garvey S. Energy storage capacity vs. renewable penetration: a study for the UK. Renew Energy 2021;171:849–67.

[10] Peters JF, Baumann M, Zimmermann B, Braun J, Weil M. The environmental impact of Li-Ion batteries and the role of key parameters–A review. Renew Sustain Energy Rev 2017;67:491–506.

[11] Wang W, Li Y, Shi M, Song Y. Optimization and control of battery-flywheel compound energy storage system during an electric vehicle braking. Energy 2021;226:120404.

[12] Schiemann M, Böhm B, Chirone R, Senneca O, Ströhle J, Umeki K, et al. Technical solutions to foster the global energy transition: special issue on clean fuel conversion technologies for carbon dioxide and pollutant reduction. Elsevier; 2022.

[13] Zhang S, Chen W. Assessing the energy transition in China towards carbon neutrality with a probabilistic framework. Nat Commun 2022;13:1–15.

[14] Ishraque MF, Shezan SA, Rashid M, Bhadra AB, Hossain MA, Chakrabortty RK, et al. Techno-economic and power system optimization of a renewable rich islanded microgrid considering different dispatch strategies. IEEE Access 2021;9:77325–40.

[15] Tovar-Facio J, Guerras LS, Ponce-Ortega JM, Martin M. Sustainable energy transition considering the water–energy nexus: a multiobjective optimization framework. ACS Sustain Chem Eng 2021;9:3768–80.

[16] Pratama YW, Purwanto WW, Tezuka T, McLellan BC, Hartono D, Hidayatno A, et al. Multi-objective optimization of a multiregional electricity system in an archipelagic state: the role of renewable energy in energy system sustainability. Renew Sustain Energy Rev 2017;77:423–39.

[17] Potrč S, Čuček L, Martin M, Kravanja Z. Sustainable renewable energy supply networks optimization–The gradual transition to a renewable energy system within the European Union by 2050. Renew Sustain Energy Rev 2021;146:111186.

[18] Lu T, Sherman P, Chen X, Chen S, Lu X, McElroy M. India's potential for integrating solar and on-and offshore wind power into its energy system. Nat Commun 2020;11:1–10.

[19] He G, Lin J, Sifuentes F, Liu X, Abhyankar N, Phadke A. Rapid cost decrease of renewables and storage accelerates the decarbonization of China's power system. Nat Commun 2020;11:1–9.

[20] Rinaldi KZ, Dowling JA, Ruggles TH, Caldeira K, Lewis NS. Wind and solar resource droughts in California highlight the benefits of long-term storage and integration with the western interconnect. Environ Sci Technol 2021;55:6214–26.

[21] Sasse J-P, Trutnevyte E. Regional impacts of electricity system transition in Central Europe until 2035. Nat Commun 2020;11:1–14.

[22] Cole WJ, Greer D, Denholm P, Frazier AW, Machen S, Mai T, et al. Quantifying the challenge of reaching a 100% renewable energy power system for the United States. Joule 2021;5:1732–48.

[23] Blanco H, Nijs W, Ruf J, Faaij A. Potential of Power-to-Methane in the EU energy transition to a low carbon system using cost optimization. Appl Energy 2018;232:323–40.

[24] Elberry AM, Thakur J, Veysey J. Seasonal hydrogen storage for sustainable renewable energy integration in the electricity sector: a case study of Finland. J Energy Storage 2021;44:103474.

[25] Vidal-Amaro JJ, Østergaard PA, Sheinbaum-Pardo C. Optimal energy mix for transitioning from fossil fuels to renewable energy sources–The case of the Mexican electricity system. Appl Energy 2015;150:80–96.

[26] Tian X, You F. Carbon-neutral hybrid energy systems with deep water source cooling, biomass heating, and geothermal heat and power. Appl Energy 2019;250:413–32.

[27] Ajagekar A, You F. Quantum computing and quantum artificial intelligence for renewable and sustainable energy: a emerging prospect towards climate neutrality. Renew Sustain Energy Rev 2022;165:112493.

[28] Ahmad T, Zhang D. Renewable energy integration/techno-economic feasibility analysis, cost/benefit impact on islanded and grid-connected operations: a case study. Renew Energy 2021;180:83–108.

[29] Jenkins JD, Zhou Z, Ponciroli R, Vilim R, Ganda F, de Sisternes F, et al. The benefits of nuclear flexibility in power system operations with renewable energy. Appl Energy 2018;222:872–84.

[30] Weitemeyer S, Kleinhans D, Vogt T, Agert C. Integration of renewable energy sources in future power systems: the role of storage. Renew Energy. 2015;75:14–20.

[31] Zhao N, You F. Toward carbon-neutral electric power systems in the New York State: a novel multi-scale bottom-up optimization framework coupled with machine learning for capacity planning at hourly resolution. ACS Sustain Chem Eng 2022;10:1805–21.

[32] Diéguez MS, Fattahi A, Sijm J, España GM, Faaij A. Modelling of decarbonisation transition in national integrated energy system with hourly operational resolution. Adv Appl Energy 2021;3:100043.

[33] McPherson M, Stoll B. Demand response for variable renewable energy integration: a proposed approach and its impacts. Energy 2020;197:117205.

[34] Brown PR, Botterud A. The value of inter-regional coordination and transmission in decarbonizing the US electricity system. Joule 2021;5:115–34.

[35] Kotzur L, Nolting L, Hoffmann M, Groß T, Smolenko A, Priesmann J, et al. A modeler's guide to handle complexity in energy systems optimization. Adv Appl Energy 2021;4:100063.

[36] Murrant D, Radcliffe J. Assessing energy storage technology options using a multi-criteria decision analysis-based framework. Appl Energy 2018;231:788–802.

[37] Wu Y, Zhang T, Gao R, Wu C. Portfolio planning of renewable energy with energy storage technologies for different applications from electricity grid. Appl Energy 2021;287:116562.

[38] Campos-Guzmán V, García-Cáscales MS, Espinosa N, Urbina A. Life cycle analysis with multi-criteria decision making: a review of approaches for the sustainability evaluation of renewable energy technologies. Renew Sustain Energy Rev 2019;104:343–66.

[39] Solangi YA, Longsheng C, Shah SAA. Assessing and overcoming the renewable energy barriers for sustainable development in Pakistan: an integrated AHP and fuzzy TOPSIS approach. Renew Energy 2021;173:209–22.

[40] Javed MS, Ma T, Jurasz J, Amin MY. Solar and wind power generation systems with pumped hydro storage: review and future perspectives. Renew Energy 2020;148:176–92.

[41] Lee HC, Chang CT. Comparative analysis of MCDM methods for ranking renewable energy sources in Taiwan. Renew Sustain Energy Rev 2018;92:883–96.

[42] Daim TU, Li X, Kim J, Simms S. Evaluation of energy storage technologies for integration with renewable electricity: quantifying expert opinions. Environ Innov Soc Transit 2012;3:29–49.

[43] Tang Y, You F. Multicriteria environmental and economic analysis of municipal solid waste incineration power plant with carbon capture and separation from the life-cycle perspective. ACS Sustain Chem Eng 2018;6:937–56.

[44] Baumann M, Weil M, Peters JF, Chibeles-Martins N, Moniz AB. A review of multi-criteria decision making approaches for evaluating energy storage systems for grid applications. Renew Sustain Energy Rev 2019;107:516–34.

[45] Walker SB, Mukherjee U, Fowler M, Elkamel A. Benchmarking and selection of Power-to-Gas utilizing electrolytic hydrogen as an energy storage alternative. Int J Hydrog Energy 2016;41:7717–31.

[46] Zhang Z, Ding T, Zhou Q, Sun Y, Qu M, Zeng Z, et al. A review of technologies and applications on versatile energy storage systems. Renew Sustain Energy Rev 2021;148:111263.

[47] Ullah Z, Wang S, Radosavljević J, Lai J. A solution to the optimal power flow problem considering WT and PV generation. IEEE Access 2019;7:46763–72.

[48] Power trends report. New York independent system operator; 2022.

[49] Zhao N, You F. New York State's 100% renewable electricity transition planning under uncertainty using a data-driven multistage adaptive robust optimization approach with machine-learning. Adv Appl Energy 2021;2:100019.

[50] Sun L, You F. Machine learning and data-driven techniques for the control of smart power generation systems: an uncertainty handling perspective. Engineering 2021;7:1239–47.

[51] Olabi A, Onumaegbu C, Wilberforce T, Ramadan M, Abdelkareem MA, Al–Alami AH. Critical review of energy storage systems. Energy. 2021;214:118987.

[52] Luo X, Wang J, Dooner M, Clarke J. Overview of current development in electrical energy storage technologies and the application potential in power system operation. Appl Energy 2015;137:511–36.

[53] Zakeri B, Syri S. Electrical energy storage systems: a comparative life cycle cost analysis. Renew Sustain Energy Rev 2015;42:569–96.

[54] Zhao S, You F. Comparative life-cycle assessment of Li-ion batteries through process-based and integrated hybrid approaches. ACS Sustain Chem Eng 2019;7:5082–94.

[55] Tao Y, Rahn CD, Archer LA, You F. Second life and recycling: energy and environmental sustainability perspectives for high-performance lithium-ion batteries. Sci Adv 2021;7.

[56] Rahman MM, Oni AO, Gemechu E, Kumar A. The development of techno-economic models for the assessment of utility-scale electro-chemical battery storage systems. Appl Energy 2021;283:116343.

[57] Kebede AA, Kalogiannis T, Van Mierlo J, Berecibar M. A comprehensive review of stationary energy storage devices for large scale renewable energy sources grid integration. Renew Sustain Energy Rev 2022;159:112213.

[58] Park J, Lee I, You F, Moon I. Economic process selection of liquefied natural gas regasification: power generation and energy storage applications. Ind Eng Chem Res 2019;58:4946–56.

[59] Lee I, You F. Systems design and analysis of liquid air energy storage from liquefied natural gas cold energy. Appl Energy 2019;242:168–80.

[60] Load & Capacity Data Gold Book. New York independent system operator; 2022.

[61] New York State Electric System Map. New York independent system operator; 2019.

[62] Energy Market & Operational Data. New York independent system operator, 2023.

[63] Clean Energy Standard. New York State energy research and development authority, 2023.

[64] Cost projections for utility-scale battery storage: 2021 update. National Renewable Energy Laboratory; 2021.

[65] Pehl M, Arvesen A, Humpenöder F, Popp A, Hertwich EG, Luderer G. Understanding future emissions from low-carbon power systems by integration of life-cycle assessment and integrated energy modelling. Nat Energy 2017;2:939–45.

[66] Shim JW, Cho Y, Kim S-J, Min SW, Hur K. Synergistic control of SMES and battery energy storage for enabling dispatchability of renewable energy sources. IEEE Trans Appl Supercond 2013;23:5701205.

[67] Ning C, You F. Data-driven adaptive robust unit commitment under wind power uncertainty: a Bayesian nonparametric approach. IEEE Trans Power Syst 2019;34:2409–18.

[68] Wei W, Liu F, Mei S. Dispatchable region of the variable wind generation. IEEE Trans Power Syst. 2014;30:2755–65.

[69] Ye H, Wang J, Ge Y, Li J, Li Z. Robust integration of high-level dispatchable renewables in power system operation. IEEE Trans Sustain Energy 2016;8:826–35.

[70] Emmanuel M, Rayudu R. Evolution of dispatchable photovoltaic system integration with the electric power network for smart grid applications: a review. Renew Sustain Energy Rev 2017;67:207–24.

[71] Zhao N, You F. Can renewable generation, energy storage and energy efficient technologies enable carbon neutral energy transition? Appl Energy 2020;279:115889.

[72] Lee I, Tester JW, You F. Systems analysis, design, and optimization of geothermal energy systems for power production and polygeneration: state-of-the-art and future challenges. Renew Sustain Energy Rev 2019;109:551–77.

[73] Tian X, Meyer T, Lee H, You F. Sustainable design of geothermal energy systems for electric power generation using life cycle optimization. AlChE J 2020;66:e16898.

[74] Niaz H, Shams MH, Liu JJ, You F. Mining bitcoins with carbon capture and renewable energy for carbon neutrality across states in the USA. Energy Environ Sci 2022;15:3551–70.

[75] Ning C, You F. Deep learning based distributionally robust joint chance constrained economic dispatch under wind power uncertainty. IEEE Trans Power Syst 2022;37:191–203.

[76] Walawalkar R, Apt J, Mancini R. Economics of electric energy storage for energy arbitrage and regulation in New York. Energy Policy 2007;35:2558–68.

[77] Adamson S, Noe T, Parker G. Efficiency of financial transmission rights markets in centrally coordinated periodic auctions. Energy Econ 2010;32:771–8.

[78] Yue D, Slivinsky M, Sumpter J, You F. Sustainable design and operation of cellulosic bioelectricity supply chain networks with life cycle economic, environmental, and social optimization. Ind Eng Chem Res 2014;53:4008–29.

[79] Zhao H, Guo S, Zhao H. Comprehensive assessment for battery energy storage systems based on fuzzy-MCDM considering risk preferences. Energy 2019;168:450–61.

[80] Brown T., Hörsch J., Schlachtberger D. PyPSA: python for power system analysis. arXiv preprint 2017.

[81] 2019 CARIS Report. New York independent system operator; 2019.

[82] 70x30 RE Buildout Base Load. New York independent system operator; 2019.

[83] Pandapower basic standard types. Pandapower.

[84] Gutman R, Marchenko P, Dunlop R. Analytical development of loadability characteristics for EHV and UHV transmission lines. IEEE Trans Power Appar Syst 1979:606–17.

[85] Kamath D, Arsenault R, Kim HC, Anctil A. Economic and environmental feasibility of second-life lithium-ion batteries as fast-charging energy storage. Environ Sci Technol 2020;54:6878–87.

[86] Baars J, Domenech T, Bleischwitz R, Melin HE, Heidrich O. Circular economy strategies for electric vehicle batteries reduce reliance on raw materials. Nat Sustain 2021;4:71–9.

[87] 2021-2040 System & Resource Outlook (The Outlook). New York independent system operator; 2022.

[88] Qiu H, Gu W, You F. Bilayer distributed optimization for robust microgrid dispatch with coupled individual-collective profits. IEEE Trans Sustain Energy 2021;12:1525–38.

[89] Ren J. Sustainability prioritization of energy storage technologies for promoting the development of renewable energy: a novel intuitionistic fuzzy combinative distance-based assessment approach. Renew Energy 2018;121:666–76.

[90] Koohi-Fayegh S, Rosen MA. A review of energy storage types, applications and recent developments. J Energy Storage 2020;27:101047.

[91] Rahman MM, Oni AO, Gemechu E, Kumar A. Assessment of energy storage technologies: a review. Energy Convers Manage 2020;223:113295.

[92] He W, King M, Luo X, Dooner M, Li D, Wang J. Technologies and economics of electric energy storages in power systems: review and perspective. Adv Appl Energy 2021;4:100060.

[93] Das CK, Bass O, Kothapalli G, Mahmoud TS, Habibi D. Overview of energy storage systems in distribution networks: placement, sizing, operation, and power quality. Renew Sustain Energy Rev 2018;91:1205–30.

[94] Wong LA, Ramachandramurthy VK, Taylor P, Ekanayake J, Walker SL, Padmanaban S. Review on the optimal placement, sizing and control of an energy storage system in the distribution network. J Energy Storage 2019;21:489–504.

[95] Tan KM, Babu TS, Ramachandaramurthy VK, Kasinathan P, Solanki SG, Raveendran SK. Empowering smart grid: a comprehensive review of energy storage technology and application with renewable energy integration. J Energy Storage 2021;39:102591.

[96] Faisal M, Hannan MA, Ker PJ, Hussain A, Mansor MB, Blaabjerg F. Review of energy storage system technologies in microgrid applications: issues and challenges. IEEE Access 2018;6:35143–64.

[97] Nadeem F, Hussain SS, Tiwari PK, Goswami AK, Ustun TS. Comparative review of energy storage systems, their roles, and impacts on future power systems. IEEE Access 2018;7:4555–85.

[98] Zhang J, Zhang Q. Feasibility and simulation study of high-rise building Micro-grid with PV and mini-hydro pumping. In: Proceedings of the IEEE power & energy society general meeting. IEEE; 2013. p. 1–5.

[99] Opitz A, Badami P, Shen L, Vignarooban K, Kannan AM. Can Li-Ion batteries be the panacea for automotive applications? Renew Sustain Energy Rev 2017;68:685–92.

[100] Demirhan CD, Tso WW, Powell JB, Heuberger CF, Pistikopoulos EN. A multiscale energy systems engineering approach for renewable power generation and storage optimization. Ind Eng Chem Res 2020;59:7706–21.

[101] Li M, Yang J, Liang S, Hou H, Hu J, Liu B, et al. Review on clean recovery of discarded/spent lead-acid battery and trends of recycled products. J Power Sources 2019;436:226853.

[102] Ridha HM, Gomes C, Hazim H, Ahmadipour M. Sizing and implementing off-grid stand-alone photovoltaic/battery systems based on multi-objective optimization and techno-economic (MADE) analysis. Energy 2020;207:118163.

[103] Dhundhara S, Verma YP, Williams A. Techno-economic analysis of the lithium-ion and lead-acid battery in microgrid systems. Energy Convers Manage 2018;177:122–42.

[104] Hydrogen. The New York State energy research and development authority.

[105] Singla MK, Nijhawan P, Oberoi AS. Hydrogen fuel and fuel cell technology for cleaner future: a review. Environ Sci Pollut Res 2021;28:15607–26.

[106] McPherson M, Johnson N, Strubegger M. The role of electricity storage and hydrogen technologies in enabling global low-carbon energy transitions. Appl Energy 2018;216:649–61.

[107] Chen X, Xie Q, Bian X, Shen B. Energy-saving superconducting magnetic energy storage (SMES) based interline DC dynamic voltage restorer. CSEE J Power Energy Syst 2021;8:238–48.

[108] Khalid M. A review on the selected applications of battery-supercapacitor hybrid energy storage systems for microgrids. Energies 2019;12:4559.

[109] Fan X, Liu B, Liu J, Ding J, Han X, Deng Y, et al. Battery technologies for grid-level large-scale electrical energy storage. Trans Tianjin Univ 2020;26:92–103.

[110] Alotto P, Guarnieri M, Moro F. Redox flow batteries for the storage of renewable energy: a review. Renew Sustain Energy Rev 2014;29:325–35.

[111] Choudhury S. Flywheel energy storage systems: a critical review on technologies, applications, and future prospects. Int Trans Electr Energy Syst 2021;31:e13024.

[112] Bazdar E, Sameti M, Nasiri F, Haghighat F. Compressed air energy storage in integrated energy systems: a review. Renew Sustain Energy Rev 2022;167:112701.

[113] Alirahmi SM, Razmi AR, Arabkoohsar A. Comprehensive assessment and multi-objective optimization of a green concept based on a combination of hydrogen and compressed air energy storage (CAES) systems. Renew Sustain Energy Rev 2021;142:110850.

[114] Storage futures study: storage technology modeling input data report. National Renewable Energy Laboratory; 2021.

[115] Argyrou MC, Christodoulides P, Kalogirou SA. Energy storage for electricity generation and related processes: technologies appraisal and grid scale applications. Renew Sustain Energy Rev 2018;94:804–21.

[116] Wind integraiton national dataset toolkit. National Renewable Energy Laboratory.